Assessing uncertainties of a geophysical approach to estimate surface fine particulate matter distributions from satellite observed aerosol optical depth

5 Xiaomeng Jin[1], Arlene M. Fiore[1], Gabriele Curci[2,3], Alexei Lyapustin[4], Kevin Civerolo[5], Michael Ku[5], Aaron van Donkelaar[6], Randall V. Martin[6,7]

1. Department of Earth and Environmental Sciences of Lamont-Doherty Earth Observatory and Columbia University, Palisades, NY, USA

2. Department of Physical and Chemical Sciences, University of L'Aquila, L'Aquila, Italy

10   3. CETEMPS, University of L'Aquila, L'Aquila, Italy

4. NASA Goddard Space Flight Center, MD, USA

5. New York State Department of Environmental Conservation, Albany, NY, USA

6. Department of Physics and Atmospheric Science, Dalhousie University, NS, Canada

7. Smithsonian Astrophysical Observatory, Harvard-Smithsonian Center for Astrophysics, Cambridge, MA, USA

Corresponding Author's Email Address: xjin@ldeo.columbia.edu

Abstract

Health impact analyses are increasingly tapping the broad spatial coverage of satellite aerosol optical depth (AOD) products to estimate human exposure to fine particulate matter ($PM_{2.5}$). We use a forward geophysical approach to derive ground-level $PM_{2.5}$ distributions from satellite AOD at 1 km^2 resolution for 2011 over the Northeast USA by applying relationships between surface $PM_{2.5}$ and column AOD (calculated offline from speciated mass distributions) from a regional air quality model (CMAQ; 12×12 km^2 horizontal resolution). Seasonal average satellite-derived $PM_{2.5}$ reveals more spatial detail and best captures observed surface $PM_{2.5}$ levels during summer. At the daily scale, however, satellite-derived $PM_{2.5}$ is not only subject to measurement uncertainties from satellite instruments, but more importantly, to uncertainties in the relationship between surface $PM_{2.5}$ and column AOD. Using 11 ground-based AOD measurements within 10 km of surface $PM_{2.5}$ monitors, we show that uncertainties in modeled $PM_{2.5}$/AOD can explain more than 70% of the spatial and temporal variance in the total uncertainty in daily satellite-derived $PM_{2.5}$ evaluated at $PM_{2.5}$ monitors. This finding implies that a successful geophysical approach to deriving daily $PM_{2.5}$ from satellite AOD requires model skill at capturing day-to-day variations in $PM_{2.5}$/AOD relationships. Overall, we estimate that uncertainties in the modeled $PM_{2.5}$/AOD lead to an error of 11 $\mu g/m^3$ in daily satellite-derived $PM_{2.5}$, and uncertainties in satellite AOD lead to an error of 8 $\mu g/m^3$. Using multi-platform ground, airborne and radiosonde measurements, we show that uncertainties of modeled $PM_{2.5}$/AOD are mainly driven by model uncertainties in aerosol column mass and speciation, while model representation of relative humidity and aerosol vertical profile shape contribute some systematic biases. The parameterization of aerosol optical properties, which determines the mass-extinction efficiency, also contributes to random uncertainty, with the size distribution the largest source of uncertainty, and hygroscopicity of inorganic salt the second.

Future efforts to reduce uncertainty in geophysical approaches to derive surface $PM_{2.5}$ from satellite AOD would thus benefit from improving model representation of aerosol vertical distribution and aerosol optical properties, to narrow uncertainty in satellite-derived $PM_{2.5}$.

Keywords: $PM_{2.5}$, aerosol optical depth, CMAQ, DISCOVER-AQ, aerosol size distribution,

5   aerosol hygroscopic growth.

1   Introduction

Exposure to ambient fine particulate matter ($PM_{2.5}$) is estimated to cause more than 8 million attributable deaths worldwide in 2015 (Burnett et al., 2018), and is associated with an increase in the risk of cardiovascular and respiratory disease (Dominici et al., 2006; Peng et al., 2009). Evidence is emerging that exposure to $PM_{2.5}$ has adverse health effects even at low concentrations (Crouse et al., 2012; Shi et al., 2015). Early studies relied on the nearest ground-based monitors to estimate $PM_{2.5}$ exposure (e.g. Dockery et al., 1993; Laden et al., 2006), but lack of resolution of spatial and temporal gradients in population exposure may lead to substantial errors in health impact analyses.

Satellite remote sensing, which fills a spatial gap in ground-based networks, is playing an increasingly important role in $PM_{2.5}$ exposure assessment (Cohen et al., 2017; Jerrett et al., 2017). Aerosol optical depth (AOD), a measure of the sum of light extinction by aerosols within the atmospheric column, is retrieved from a number of satellite instruments. The Moderate Resolution Imaging Spectroradiometer (MODIS) on board Terra and Aqua has provided twice-daily global AOD data for nearly two decades, and the Multi-Angle Implementation of Atmospheric Correction (MAIAC) product has refined the spatial resolution retrieved from MODIS to 1 km (Lyapustin et al., 2011; 2012; 2018), offering the potential to reveal aerosol spatial variability within urban cores (Hu et al., 2014). A big challenge to inferring near-surface $PM_{2.5}$ from column AOD retrieved from satellite instruments is to describe accurately the non-linear and spatiotemporally varying relationship between $PM_{2.5}$ and AOD, which depends on aerosol chemical composition, vertical profiles, aerosol optical properties and the ambient environment (Griffin et al., 2012). Approaches to link satellite AOD with $PM_{2.5}$ exposures are often classified into two categories: statistical (e.g. Di et al., 2016; Hu et al., 2014; Kloog et al., 2014) and geophysical (e.g. van Donkelaar et al.,

2010; 2006). A two-stage process is also used with a geophysical approach followed by a statistical approach (e.g. van Donkelaar et al., 2015; de Hoogh et al., 2016; Shaddick et al., 2017).

Statistical approaches fit an optimized relationship between ground-based $PM_{2.5}$ and satellite AOD along with other predictors (e.g. land use, meteorology, traffic density etc.) using

5   methods such as multiple linear regression (e.g. Gupta and Christopher, 2009; Lee et al., 2016), geographic regression (Hu et al., 2014), generalized additive models (e.g. Kloog et al., 2014), or machine learning (Di et al., 2016). In regions with high monitor density, the statistical methods generally agree better with ground-based observations than $PM_{2.5}$ derived with geophysical approach, but statistical methods rely on the availability of ground-based monitors to train the

10   statistical model, and are thus limited to regions with dense monitoring networks.

The geophysical approach that has been applied to AOD is a process-based forward approach that uses chemical transport models to explicitly simulate the spatially and temporally varying relationship between column AOD and $PM_{2.5}$ (van Donkelaar et al., 2006). The satellite-derived $PM_{2.5}$ is calculated by taking the product of satellite AOD with the modeled ratio of $PM_{2.5}$

15   to AOD (van Donkelaar et al., 2006):

$$PM_{2.5\_sat} = AOD_{sat} \times \frac{PM_{2.5\_model}}{AOD_{model}} \tag{1}$$

This geophysical approach has the advantage of broad spatial coverage that is not limited by the availability of *in-situ* measurements (van Donkelaar et al., 2006), and thus has been integral for studying the global burden of disease attributable to ambient air pollution (Cohen et al., 2017).

20   Van Donkelaar et al. (2010) estimate global annual average $PM_{2.5}$ using AOD observed from both MODIS and MISR (Multiangle Imaging Spectroradiometer) by $PM_{2.5}$-AOD relationships from a global chemical transport model (GEOS-Chem). They estimate an overall uncertainty of around

25% for annual average satellite-derived $PM_{2.5}$, but the uncertainty of the geophysical approach on short-time scales is expected to be larger (van Donkelaar et al., 2012).

The overall uncertainty in deriving surface $PM_{2.5}$ with the geophysical approach consists of uncertainty in the satellite AOD as well as the modeled $PM_{2.5}$/AOD. First, satellite observations of AOD are subject to uncertainties due to the viewing geometry, the presence of clouds and snow, and choices involved in modeling optical aerosol and surface properties (Superczynski et al., 2017; Toth et al., 2014). Second, since the relationship between $PM_{2.5}$ and AOD is non-linear and multivariate, modeled $PM_{2.5}$/AOD is subject to model uncertainties in aerosol vertical distributions, aerosol speciation and the ambient environment. Third, even if a model simulates accurately the aerosol mass distribution, calculating AOD in models generally requires assumptions regarding the aerosol size distribution, aerosol species density, refractive index and hygroscopic growth factors, all of which are sources of uncertainties (Curci et al., 2015). The ability of a particle to scatter and absorb light largely depends on its size, which varies significantly in nature (Stanier et al., 2004). As resolving the size distribution is computationally expensive (Adams, 2002), aerosols are typically assumed to follow a certain distribution (e.g. log-normal), which can introduce error. Moreover, aerosol water uptake (hygroscopicity) affects the aerosol size and optical properties, but the representation of hygroscopic factors in models varies considerably (Chin et al., 2002; Curci et al., 2015; Drury et al., 2010). The hygroscopic growth factor for organic carbon (OC) is especially uncertain, varying by organic species, and is poorly represented in models (Ming et al., 2005; Jimenez et al., 2009; Latimer and Martin, 2018). The impacts of these uncertainties on aerosol radiative forcing have been studied extensively, but their impacts on deriving surface $PM_{2.5}$ from satellite-based column AOD have not yet been quantified.

Here, we estimate $PM_{2.5}$ distributions over the Northeast USA for 2011 using a geophysical approach that combines MAIAC AOD data with modeled $PM_{2.5}$/AOD relationships simulated with a regional air quality model (CMAQ). Compared to the global GEOS-Chem model used by van Donkelaar et al. (2016), CMAQ has finer spatial resolution (12×12 km^2) and a locally refined emission inventory (see Sect. 2.2). We use an ensemble of surface (AQS, AERONET, IMPROVE, CSN), aircraft (DISCOVER-AQ) and radiosonde (IGRA) measurements to evaluate different sources of uncertainties in satellite-derived $PM_{2.5}$, especially at the daily scale. To evaluate the sensitivities of satellite-derived $PM_{2.5}$ to the parameterization of aerosol optical properties, we conduct a series of sensitivity tests in an offline AOD calculation package (FlexAOD). The overarching goal of the comprehensive uncertainty analysis is to assess the relative importance of each uncertain factor, thereby advancing the process-level understanding of the relationship between satellite AOD and surface $PM_{2.5}$ air quality.

2   Data and methods

2.1   Satellite AOD products

We use the high-resolution (1 km) daily AOD products retrieved from the MODIS instruments onboard the Terra and Aqua satellites with the MAIAC algorithm, which applies time series analysis and image processing techniques (Lyapustin et al., 2011; 2018a, b). The spatial resolution of MAIAC (1 km) is finer than the conventional MODIS Dark Target and Deep Blue AOD products (10 km). The MAIAC algorithm improved upon the earlier Dark Target retrieval algorithm (MOD04) by explicitly including bi-directional reflectance (rather than the parameterized Dark Target approach), which improves accuracy over brighter surfaces, with similar accuracy over dark and vegetated surfaces (Lyapustin et al., 2011).

Using the quality flags provided, we filtered out pixels with or adjacent to cloud, snow or ice. We follow the approach of Hu et al. (2014) to combine daily MAIAC AOD from Terra (overpasses around 10:30 AM local time) and Aqua (overpasses around 1:30 PM local time). For the pixels where both Terra and Aqua have valid data, we take the average to reflect the mean daytime AOD. For pixels where only one instrument has valid data, AOD may be biased accordingly towards morning or afternoon conditions. We find, on average, Terra-MAIAC AOD is higher than Aqua-MAIAC AOD by 0.005 (about 5% of the annual average AOD) over the Northeast USA in 2011, reflecting diurnal variations of AOD (Green et al., 2012) and potential calibration differences (Levy et al., 2018). To account for these differences, we fit two linear equations (R = 0.87) between Terra-MAIAC (AOD_T) and Aqua-MAIAC AOD (AOD_A):

$$\widehat{AOD_T} = 0.84 AOD_A + 0.019 \qquad (2)$$

$$\widehat{AOD_A} = 0.88 AOD_T + 0.005 \qquad (3)$$

We use Eq. (2) and (3) to predict the AOD from the other instrument when one of them is missing, and then take the average. We find little seasonal variation in the linear relationship.

2.2 CMAQ model

The Community Multiscale Air Quality Modeling System (CMAQ) is a regional multipollutant air quality model developed and maintained by the U.S. Environmental Protection Agency (EPA). We use the CMAQ (v5.0.2) model simulations for 2011 conducted at New York State Department of Environmental Conservation (NYSDEC) for air quality planning purposes. The simulations are conducted for the eastern USA with 12 km horizontal resolution and 35 vertical layers extending up to 50 hPa. The meteorological fields to drive CMAQ are provided by annual Weather Research and Forecast (WRF) v3.4 model simulations over continental United States. Chemical boundary conditions are from the GEOS-Chem (2° × 2.5°) global chemical

transport model (Bey et al., 2001, version 8) generated by EPA. The emission inventory is based on the 2011 National Emission Inventory (NEI) and processed through the Sparse Matrix Operator Kernel Emissions (SMOKE; (Houyoux et al., 2000)). Biogenic emissions are generated with the Biogenic Emissions Inventory System (BEIS) v3.61 (Pierce et al., 2002). Prescribed burning and

5 wildfire emissions are computed using the SmartFire 2 (Raffuse et al., 2009). Mobile emissions are produced from the EPA's MOtor Vehicle Emission Simulator (MOVES) 2014a (US EPA, MOVES2014a). The gas-phase chemical mechanism is CB05, and the aerosol module is AERO6. Appel et al. (2013; 2017) provide details on the calculation of total $PM_{2.5}$ mass and speciated aerosol mass, as well as model evaluation.

10 **2.3 Offline AOD calculation**

We calculate hourly AOD from the CMAQ model (AOD_{CMAQ}) offline from the archived hourly, three-dimensional, speciated aerosol (i.e. sulfate, nitrate, ammonium, black carbon, organic carbon, sea salt, soil dust) distribution and meteorological fields (i.e. relative humidity, hereafter RH) using the Flexible Aerosol Optical Depth (FlexAOD) post-processing tool.

15 FlexAOD was originally developed to calculate aerosol optical properties for the GEOS-Chem model. It is based on the NASA Codes for Computation of Bidirectional Reflectance of Flat Particulate Layers and Rough Surfaces (Mishchenko et al., 1999). We adapt FlexAOD to CMAQ by matching the aerosol speciation with GEOS-Chem based on Appel et al. (2013). Under the assumption of spherical particles, aerosol optical properties are calculated based on Mie theory.

20 Given size distributions for each aerosol species, aerosol light extinction (EXT_l) at a given model layer is calculated as follows (Curci, 2015):

$$EXT_l = \sum_{i=1}^{N} \frac{3}{4} \frac{\overline{Q_{e,dry,i} f_{RH_l,i}}}{r_{e,dry,i} \rho_i} M_{i,l} \tag{4}$$

where i refers to the species, N is the number of aerosol species ($N = 5$: sulfate-nitrate-ammonium (SNA), OC, black carbon (BC), dust, sea salt), $\overline{Q_{e,dry,\iota}}$ is the Mie extinction efficiency of species i averaged over the dry size distribution, $f_{RH_l,i}$ is the hygroscopic growth factor of species i at given RH_l, ρ_i is aerosol density of species i, $M_{i,l}$ is the aerosol mass of species i at layer l, and

5    $r_{e,dry,i}$ is the dry effective radius. AOD_{CMAQ} is then calculated as the vertical integral of EXT_l across all model layers:

$$AOD_{CMAQ} = \int_{l=1}^{L} EXT_l \, dz \tag{5}$$

We use the recommended values of Drury et al. (2010) for aerosol density. The refractive index (m) in the default run is adapted from the Optical Properties of Aerosols and Clouds (OPAC)

10   database (Hess et al., 1998). As CMAQ does not explicitly simulate the size distribution of aerosols, we assume log-normal distributions for all species except for dust (assumed to be a gamma distribution). The effective radius (r_e), or the area-weighted mean radius of log-normal size distribution can be derived as:

$$r_{e,dry,i} = r_0 e^{\left(\frac{5}{2}ln^2\sigma_g\right)} \tag{6}$$

15   where r_0 is the specific modal radius, σ_g is the geometric standard deviation. For the aerosol size distribution and density, we follow the recommended values of Drury et al. (2010) in the default run. We apply the single parameter κ to represent the hygroscopic growth of SNA and organic carbon, as developed by Petters and Kreidenweis (2007) based on the κ-Kohler theory, which is the most commonly used function in the literature (Brock et al., 2016; Snider 2016). The

20   hygroscopic growth factor can be simplified as a function of parameter κ and RH (Snider et al., 2016):

$$f(RH) = (1 + \kappa \frac{RH}{100-RH})^{1/3} \tag{7}$$

Koehler et al. (2006) suggest κ for SNA (κ_{SNA}) ranges from 0.33 to 0.72, with a mean of 0.53. The hygroscopic growth factor of organic carbon (κ_{oc}) varies with species and is correlated with the age of organics (Duplissy et al., 2011). Duplissy et al. (2011) and Jimenez et al. (2009) suggest κ for organic carbon typically ranges from 0 to 0.2. We apply $\kappa_{SNA} = 0.53$, and $\kappa_{oc} = 0.1$. For black carbon and sea salt, we apply the hygroscopic growth factors reported in Chin et al. (2002). In addition to the default values, we test the sensitivities of the derived $PM_{2.5}$ to uncertainties in aerosol optical property parameterization by varying each parameter across a range of values reported in the literature, as specified in Table 1.

2.4 Ground-based observations

AErosol RObotic NETwork (AERONET) is a federated instrument network that provides ground-based information about aerosols including AOD, derived from sun photometer measurements of direct solar radiation (Holben et al., 1998). We use Level-2 (cloud screened and quality assured) daily average data from 13 sites over the Northeast USA. We also include observed AOD from the Distributed Regional Aerosol Gridded Observation Networks (DRAGON)-USA 2011 field campaign, co-located with the DISCOVER-AQ aircraft campaign. The DRAGON campaign provides extensive sun photometer measurements of AOD at 38 sites along the flight path of DISCOVER-AQ from July 1 to August 15, 2011, which were incorporated into the AERONET database. To allow direct comparison with AOD_{MAIAC} and AOD_{CMAQ}, AERONET AOD measurements at 0.44 μm and 0.675 μm were interpolated to 0.55 μm using the Angstrom exponent (the first derivative of AOD with wavelength, on a logarithmic scale) provided.

We use ground-based measurements of daily 24-hour average $PM_{2.5}$ from 152 EPA Air Quality System (AQS) sites over the Northeast USA. Of the 152 sites, 13 sites have AERONET sites within 10 km (about the resolution of CMAQ). We consider these 13 sites as "co-located"

and use them to evaluate uncertainties in modeled $PM_{2.5}$/AOD relationships. We also use AQS aerosol speciation data at 54 sites which include the Chemical Speciation Network (CSN) and the Interagency Monitoring of Protected Visual Environments (IMPROVE) visibility monitoring network.

5   To evaluate the modeled vertical profile of ambient RH, we use ground-based soundings from 6 radiosonde sites over the Northeast USA. Aggregated daily data at 0:00 and 12:00 UTC are acquired from the NOAA Integrated Global Radiosonde Archive (IGRA), and modeled vertical profiles are sampled concurrently with radiosonde observations. We use the RH data calculated from vapor pressure, saturation vapor pressure and ambient air pressure (Durre and Yin, 2008).

10   **2.5   NASA DISCOVER-AQ 2011 Field Campaign**

The NASA DISCOVER-AQ (Deriving Information on Surface conditions from Column and Vertically Resolved Observations Relevant for Air Quality) aircraft campaign over Baltimore-Washington, D.C. in July 2011 provides extensive, systematic, concurrent measurements of aerosol chemical, optical, and microphysical properties. The NASA P-3B aircraft performed 14
15   flights which include 247 profiles (typically extending from 0.4 to 3.2 km above the surface) over six DRAGON sites (Crumeyrolle et al., 2014). We use the simultaneous measurements of aerosol composition (SNA, OC, BC), scattering, absorption, and extinction coefficients at dry (RH<40%), ambient and wet (RH>80%) environments. To reduce the random uncertainties of individual observations and to allow direct comparison with CMAQ and ground-based observations, we
20   aggregate the daily aircraft profiles horizontally to six locations corresponding to the six sites, and vertically to CMAQ model layers, and then sample CMAQ modeled values consistently with observations.

3 Results and Discussion

3.1 Deriving surface PM$_{2.5}$ from satellite observations

We derive satellite-based PM$_{2.5}$ (hereafter PM$_{2.5\_MAIAC}$) over the Northeast USA for 2011 by taking the product of daily average CMAQ modeled PM$_{2.5}$/AOD relationships (PM$_{2.5\_CMAQ}$/AOD$_{CMAQ}$) with MAIAC AOD (AOD$_{MAIAC}$, Eq. (1)). These unconstrained PM$_{2.5}$ estimates (Fig. 1) are independent of surface observations. As PM$_{2.5\_MAIAC}$ is determined as the product of observed AOD$_{MAIAC}$ and modeled PM$_{2.5\_CMAQ}$/AOD$_{CMAQ}$, the spatial patterns of PM$_{2.5\_MAIAC}$ will be affected by the spatial variations of both AOD$_{MAIAC}$ and PM$_{2.5\_CMAQ}$/AOD$_{CMAQ}$. Fig. 1a) shows the summertime average (JJA) AOD$_{MAIAC}$ at 1km resolution overlaid with AERONET observed AOD. While we find high AOD over some populated urban areas such as New York City (NYC), high AOD$_{MAIAC}$ is also found over central New York State (NYS), away from major anthropogenic sources. In CMAQ, PM$_{2.5}$ (PM$_{2.5\_CMAQ}$) occurs over regions with major anthropogenic sources such as NYC. AOD$_{CMAQ}$ also shows a latitudinal dependence, with higher AOD at lower latitudes, which reflects 1) relatively high emissions of aerosol and its precursors from anthropogenic and biogenic sources over MD, PA and NYC; and 2) latitudinal variations of RH that affect aerosol hygroscopic growth. The modeled PM$_{2.5\_CMAQ}$/AOD$_{CMAQ}$ varies spatially (one standard deviation (SD) is 45 μg/m^3 per unit of AOD), mainly driven by the spatial variations of PM$_{2.5\_CMAQ}$ (R = 0.86). We find the overall spatial pattern of satellite-derived PM$_{2.5}$ correlates more strongly with modeled PM$_{2.5\_CMAQ}$/AOD$_{CMAQ}$ (R = 0.97) than observed AOD$_{MAIAC}$ (R = 0.8), suggesting that the large-scale spatial variability reflects modeled rather than satellite-based distributions, at least under our framework for the Northeast USA in summer. The temporal variability in PM$_{2.5\_MAIAC}$ is also mainly driven by variability in PM$_{2.5\_CMAQ}$/AOD$_{CMAQ}$ (R = 0.61), with little temporal correlation between regional average

AOD_{MAIAC} and $PM_{2.5\_MAIAC}$ (R = 0.05, Fig. 2). At short time scales, the daily variability in regional average $PM_{2.5\_MAIAC}$ shows stronger correlation with $PM_{2.5\_CMAQ}/AOD_{CMAQ}$ in all seasons except for JJA, when $PM_{2.5\_MAIAC}$ are driven by variability in both AOD_{MAIAC} (R = 0.5) and $PM_{2.5\_CMAQ}/AOD_{CMAQ}$ (R = 0.4, Fig. 2). Summertime AOD_{MAIAC} is higher than wintertime AOD by 50%, while summertime $PM_{2.5\_MAIAC}$ is lower than in winter by 46%. Previous studies also found inconsistent seasonal cycles in AOD and $PM_{2.5}$ (Ford et al., 2013; Kim et al., 2015). We attribute the opposite seasonal cycle in $PM_{2.5\_MAIAC}$ and AOD_{MAIAC} to three factors: 1) weak boundary layer ventilation in winter that leads to sharp vertical gradients of aerosol distribution (Kim et al., 2015); 2) higher RH in summer that leads to larger hygroscopic growth; 3) model overestimates of $PM_{2.5}$ (especially OC) in wintertime and underestimates of $PM_{2.5}$ in summertime, leading to an overestimate of the winter-to-summer decrease in $PM_{2.5\_CMAQ}/AOD_{CMAQ}$ (see section 3.3).

While at larger spatial scales, $PM_{2.5\_CMAQ}/AOD_{CMAQ}$ contributes more to the spatial and temporal variability in $PM_{2.5\_MAIAC}$ than AOD_{MAIAC}, at smaller scales, over which we assume the spatial variability of $PM_{2.5}/AOD$ is homogenous, incorporating fine-resolution satellite data reveals stronger spatial gradients (e.g., enhancements along industrial corridors) than $PM_{2.5\_CMAQ}$ (Fig. 1b). In addition to refining spatial resolution, satellite-derived $PM_{2.5}$ can correct model summertime biases in $PM_{2.5}$. Observed AOD from AERONET and $PM_{2.5}$ from AQS indicate an overall underestimate in both AOD_{CMAQ} (Fig. 1c; normalized mean bias (NMB) = -44%) and $PM_{2.5\_CMAQ}$ (Fig. 1d; NMB= -17%) in summer. We find $PM_{2.5\_CMAQ}/AOD_{CMAQ}$ is overall consistent with the observed $PM_{2.5}/AOD$ sampled at co-located AQS-AERONET sites (NMB = 0.9%) as the ratio largely cancels out the model underestimates in both $PM_{2.5}$ and AOD. AOD distributions retrieved from MODIS (AOD_{MAIAC}) agree better with AERONET AOD than AOD_{CMAQ} (NMB =

5%, Fig. 1f), though we find small low biases at two sites in New York City and at most DRAGON sites over Maryland. Our derived distribution of $PM_{2.5\_MAIAC}$ is thus closer to $PM_{2.5}$ observed at AQS sites than $PM_{2.5\_CMAQ}$ (NMB = 4.7% vs. 44% for $PM_{2.5\_CMAQ}$, Fig. 1g). However, the $PM_{2.5\_MAIAC}$ distribution is wider than observed at AQS: the lowest 5% is 5 versus 7 $\mu g/m^3$ for

5    $PM_{2.5\_MAIAC}$ vs. AQS $PM_{2.5}$, and the highest 5% is 16 versus 13 $\mu g/m^3$. We find that $PM_{2.5\_MAIAC}$ is biased high over New York City, coastal regions of Massachusetts, on the borders of upstate New York, and northern Vermont. Evaluation of $PM_{2.5\_MAIAC}$ in other seasons show larger biases and uncertainties (Fig. S1). In the following sections, we examine sources of uncertainties and biases in satellite-derived $PM_{2.5}$. We quantify the uncertainties in terms of bias (systematic) and

10   random uncertainty. The bias uncertainty is linked to the overall accuracy, while the random uncertainty reflects random fluctuations in the measurements or the imprecision of the model resulting from imperfect modeling assumptions and simplifications.

3.2   Evaluation of satellite observed AOD products

AOD_{MAIAC} in general agrees well with AERONET observations (spatial R= 0.83, temporal

15   R = 0.85, MB = -0.01, and RMSE =0.07). The performance of AOD_{MAIAC} evaluated at Northeast US AERONET sites is consistent with the evaluation of Superczynski et al. (2017) over North America (R = 0.82, MB = -0.008). We find, however, that AOD_{MAIAC} in winter (December-January-February, DJF) is biased high by 49% (MB = +0.02) on average. The wintertime overestimate is likely due to residual snow contamination which is below the detection limit, even

20   though we applied a stringent data quality filter to remove pixels flagged as snow. We find the wintertime overestimate is most evident over northern latitudes (e.g. AERONET sites in Massachusetts, NMB ranges from 80% to 180%), where snow occurs more often. The NMB of AOD_{MAIAC} are 15% in MAM, -5% in JJA, and 17% in SON respectively, though the quantile range

of the error is large, suggesting that single observations have large random uncertainties (Fig. 3). Taking the 1σ standard deviation of the normalized biases as a metric of random uncertainty, we estimate the uncertainties of daily satellite observations to be around 80% in DJF, 60% in MAM and SON, and 50% in JJA. Spatial and/or temporal averaging can reduce these random errors of satellite observations, which is evidenced as the smaller spread of errors than for monthly averages at the same spatial resolution, or daily data at coarser (10km) resolution, but it does not reduce the overall MB between AOD_{MAIAC} and $AOD_{AERONET}$ (Fig. 3). We find that spatially averaging AOD_{MAIAC} to 10 km leads to an overall increase of AOD_{MAIAC}. Temporal averaging, on the other hand, leads to an overall decrease in AOD_{MAIAC} except for DJF, leading to smaller positive MB in SON (7%) and MAM (7%), but larger negative MB in JJA (-8%) and positive MB (67%) in DJF.

3.3 Evaluation of modeled $PM_{2.5}$/AOD relationships

Three factors contribute to the overall uncertainty in the modeled $PM_{2.5}$/AOD relationship: 1) $PM_{2.5\_CMAQ}$; 2) AOD_{CMAQ}; 3) the relation between 1) and 2). We evaluate uncertainties of the three factors at 13 paired AQS-AERONET sites (within 10 km of each other; about the resolution of CMAQ). Figure 4 shows the distribution of the biases of modeled daily $PM_{2.5\_CMAQ}$, AOD_{CMAQ} and $PM_{2.5\_CMAQ}$/AOD_{CMAQ} compared with observations. Generally, $PM_{2.5\_CMAQ}$ biases vary seasonally: from +42% in DJF to -39% in JJA on average. In contrast, AOD_{CMAQ} biases show weaker seasonality. The normalized MBs of AOD_{CMAQ} are 3% in DJF, -16% in MAM, -7% in JJA and -20% in SON. On the daily scale, biases of AOD_{CMAQ} are weakly correlated with the biases of $PM_{2.5\_CMAQ}$ (R = 0.14), suggesting model biases in AOD do not necessarily reflect biases in modeled $PM_{2.5}$. This is in contrast with prior analysis of annual means where emission biases drive similar biases in AOD and $PM_{2.5}$ (van Donkelaar et al., 2013). The better accuracy of emissions in the Northeast USA than elsewhere in the world allows processes other than emissions to be more

important for the Northeast USA. We find the seasonal biases in modeled $PM_{2.5}$ are retained in the $PM_{2.5\_CMAQ}/AOD_{CMAQ}$ ratio, which exceeds the biases of $PM_{2.5\_CMAQ}$ in DJF, MAM and SON. As both $PM_{2.5\_CMAQ}$ and AOD_{CMAQ} are biased low in JJA, the modeled $PM_{2.5}/AOD$ bias (-20%) is smaller than that of $PM_{2.5\_CMAQ}$ (-39%). Biases in $PM_{2.5\_CMAQ}$ and AOD_{CMAQ} are oppositely signed

5   in fall, leading to the largest mean biases of modeled $PM_{2.5}/AOD$ (+74%). The spread of the biases of $PM_{2.5\_CMAQ}/AOD_{CMAQ}$ is larger than that of $PM_{2.5\_CMAQ}$ and AOD_{CMAQ}, with the standard deviation ranging from 50% in JJA to 100% in SON.

3.4   Relative importance of satellite AOD versus modeled $PM_{2.5}/AOD$ to uncertainties in satellite-derived $PM_{2.5}$

10   We have shown that both satellite AOD and modeled $PM_{2.5}/AOD$ are subject to large uncertainties at the daily time-scale. To directly compare the relative importance of the biases of satellite AOD vs. model $PM_{2.5}/AOD$ on the satellite-derived $PM_{2.5}$, we scale the biases of modeled $PM_{2.5}/AOD$ with daily AOD_{MAIAC}, so that the biases are expressed in units of $PM_{2.5}$ ($\mu g/m^3$):

$$\Delta PM_{2.5\_AOD} = (AOD_{MAIAC} - AOD_{AERONET}) \times \frac{PM_{2.5\_CMAQ}}{AOD_{CMAQ}} \qquad (8)$$

15   We then scale the biases of AOD_{MAIAC} with the daily modeled $PM_{2.5}/AOD$ relationship:

$$\Delta PM_{2.5\_Rel} = \left(\frac{PM_{2.5\_CMAQ}}{AOD_{CMAQ}} - \frac{PM_{2.5\_AQS}}{AOD_{AERONET}} \right) \times AOD_{MAIAC} \qquad (9)$$

We can also interpret $\Delta PM_{2.5\_AOD}$ and $\Delta PM_{2.5\_Rel}$ as the changes in derived $PM_{2.5}$ if we use 'true' observed AOD or $PM_{2.5}/AOD$ instead of AOD_{MAIAC} or modeled $PM_{2.5}/AOD$. As shown in Fig. 5a, mean biases caused by modeled $PM_{2.5}/AOD$ are +9.2 $\mu g/m^3$ in DJF, +2.8 $\mu g/m^3$ in MAM, -3.3

20   $\mu g/m^3$ in JJA, and +7.7 $\mu g/m^3$ in SON respectively, which introduces larger biases to the derived $PM_{2.5}$ than the MAIAC satellite product in all seasons (7.6 $\mu g/m^3$ in DJF, +1.3 $\mu g/m^3$ in MAM, -0.7 $\mu g/m^3$ in JJA, and 0.9 $\mu g/m^3$ in SON). Using the root mean squared $\Delta PM_{2.5\_AOD}$ to quantify the random uncertainty, satellite AOD contributes an overall random error of 8.3 $\mu g/m^3$ to daily

satellite $PM_{2.5\_MAIAC}$ with the smallest error in JJA (5.1 μg/m^3) and largest error in DJF (13.2 μg/m^3), while modeled $PM_{2.5}$/AOD contributes an error of 10.8 μg/m^3 (root mean squared $\Delta PM_{2.5\_Rel}$) with smallest error in JJA (6.5 μg/m^3) and largest error in SON (15.2 μg/m^3). The spread of the biases is larger for modeled $PM_{2.5}$/AOD than that for MAIAC AOD except for DJF. Our findings are consistent with Ford and Heald (2016), who use a higher-resolution (nested) version of the GEOS-Chem model and MODIS Dark Target AOD (Collection 6) to estimate two times larger uncertainties in surface $PM_{2.5}$ resulting from modeled $PM_{2.5}$/AOD relationships than in satellite AOD.

At the daily time scale, both $\Delta PM_{2.5\_AOD}$ and $\Delta PM_{2.5\_Rel}$ show large day-to-day variability: the 1σ standard deviation is 10.5 μg/m^3 for daily $\Delta PM_{2.5\_AOD}$ and 8.3 μg/m^3 or daily $\Delta PM_{2.5\_Rel}$. Next, we evaluate the dependence of the biases of satellite-derived $PM_{2.5}$ (denoted as $\Delta PM_{2.5\_MAIAC}$, evaluated with AQS observed $PM_{2.5}$) on $\Delta PM_{2.5\_Rel}$ versus $\Delta PM_{2.5\_AOD}$ by evaluating the Pearson correlation coefficients (R). Overall, $\Delta PM_{2.5\_MAIAC}$ is more strongly correlated with $\Delta PM_{2.5\_Rel}$ (R = 0.85) than that with $\Delta PM_{2.5\_AOD}$ (R = 0.53), indicating the uncertainties of modeled $PM_{2.5}$/AOD are a more important driving factor to the uncertainties of daily satellite-derived $PM_{2.5}$, which could explain 72% variance (R^2) in $\Delta PM_{2.5\_MAIAC}$. In JJA, however, $\Delta PM_{2.5\_MAIAC}$ is moderately correlated with both $\Delta PM_{2.5\_AOD}$ (R = 0.48) and $\Delta PM_{2.5\_Rel}$ (R = 0.49), suggesting uncertainties of modeled $PM_{2.5}$/AOD and satellite AOD contribute equally to the uncertainties of satellite-derived $PM_{2.5}$. We note that there is no statistically significant correlation between $\Delta PM_{2.5\_Rel}$ and $\Delta PM_{2.5\_AOD}$, with R ranging from -0.4 in SON to 0.23 in JJA, which suggests that the errors caused by modeled $PM_{2.5}$/AOD and by satellite AOD are independent of each other.

3.5 Factors leading to uncertainties in modeled PM$_{2.5}$/AOD relationship

Uncertainties in the modeled PM$_{2.5}$/AOD relationship mainly reflect uncertain aerosol speciation, aerosol vertical profiles, ambient RH, and parameterizations for aerosol optical properties including aerosol density, size distribution, refractive index and hygroscopic growth. Here we quantify the uncertainties from each factor and evaluate their impacts on the derived PM$_{2.5}$.

3.5.1 Aerosol speciation

Aerosol optical properties vary with chemical composition. Model biases in the aerosol composition also affect the overall representation of particle hygroscopicity. For the same PM$_{2.5}$ abundance, variations in the aerosol composition may alter the particle optical properties especially hygroscopicity, and consequently the PM$_{2.5}$/AOD relationship. Fig. 6a compares the modeled aerosol composition with ground-based observations averaged for each season. High biases in PM$_{2.5\_CMAQ}$ in winter are largely due to model overestimates of OC by a factor of three, and low biases in summer are due to a combination of underestimated SNA and OC. As a result, CMAQ overestimates the fraction of OC by about 20% in DJF, 15% in MAM, and less than 10% in other seasons, while underestimates the fraction of SNA by 5% to 20% in all seasons.

To estimate the impacts of model biases in aerosol speciation on AOD$_{CMAQ}$ and PM$_{2.5\_MAIAC}$, we keep the total aerosol mass the same, and redistribute AOD (AOD_{CMAQ_ir}) of each species i based on observed fraction of each species (i.e. SNA, OC, EC, soil dust; sea salt was excluded due to the limited ground-based measurements and its negligible contribution):

$$AOD_{CMAQ\_ir} = \frac{PM_{i\_obs}}{PM_{TOT\_obs}} \times \frac{PM_{TOT\_CMAQ}}{PM_{i\_CMAQ}} \times AOD_{CMAQ\_i} \qquad (10)$$

where PM_{TOT_obs} and PM_{TOT_CMAQ} are the total aerosol mass from observations and CMAQ respectively, which are reconstructed by summing up SNA, OC, EC and soil dust. Next, we estimate the uncertainty due to speciation as the differences in derived PM$_{2.5\_MAIAC}$ (ΔPM$_{2.5\_spe}$)

using the redistributed AOD_{CMAQ_ir} instead of the original AOD_{CMAQ}, shown in Fig. 6b. As SNA generally has the largest mass extinction efficiency, a low bias in SNA leads to an overall underestimate of AOD_{CMAQ}, and therefore an overestimate of $PM_{2.5\_MAIAC}$, which is largest in winter (MB = 2.2 µg/m^3, SD = 2.6 µg/m^3) and smallest in summer (MB = 0.7 µg/m^3, SD = 3.0 µg/m^3). The estimated biases due to speciation show similar seasonal cycles as the modeled $PM_{2.5}$/AOD biases (Fig. 4), suggesting that aerosol speciation errors contribute to the seasonality in modeled $PM_{2.5}$/AOD biases. Overall, model-observation discrepancy in speciation causes an error (root mean squared $\Delta PM_{2.5\_spe}$) of 4.0 µg/m^3. On a daily basis, the correlation (R) between $\Delta PM_{2.5\_spe}$ and $\Delta PM_{2.5\_MAIAC}$ is over 0.5 for all seasons except JJA, which means model biases in speciation alone can explain more than 25% variance (R^2) in $\Delta PM_{2.5\_MAIAC}$. Biases in speciation in JJA have relatively smaller impacts on the derived $PM_{2.5}$, which contribute less than 1 µg/m^3 MB and shows weak correlation with $\Delta PM_{2.5\_MAIAC}$ (R = 0.15).

3.5.2 Aerosol vertical profile

A caveat on the results in the Sect. 3.5.1 is that we assume the model errors in speciation are constant across all vertical layers, as AQS sites only provide observations near the surface. The DISCOVER-AQ aircraft campaign measured vertical variations in aerosol composition, although spatial and temporal coverage is limited. Figure 7a compares the modeled and observed vertical distributions of SNA, OC and BC averaged over the DISCOVER-AQ campaign. We do not discuss sea salt and dust here since they contribute a negligible portion of the total aerosol mass in this region. Both model and observations show SNA contributes more than half of the total aerosol across all vertical layers (Fig. 7). Aircraft observations show SNA decreases gradually with altitude with a nearly constant vertical gradient, while SNA_{CMAQ} is well mixed below 1.5 km, and starts to decline at the same rate as $SNA_{aircraft}$ above 1.5 km (Fig. 7). CMAQ underestimates SNA below

1.5 km, but overestimates SNA at higher altitudes. The positive model bias of SNA at higher altitudes may be due to excessive vertical transport, or overestimation of RH (Sect. 3.4.3) and consequently overestimation of SO_2 oxidation rate and aerosol water uptake. OC, on the other hand, is biased low at all altitudes, which is likely due to inaccurate treatment of the production of secondary organic aerosol (Zhang et al., 2009). The newer version of CMAQv5.1 shows higher SOA concentration in summer with the introduction of new SOA species (Appel et al., 2017). BC is generally low during the campaign (typically lower than 0.3 $\mu g/m^3$). BC_{CMAQ} generally agrees well with $BC_{aircraft}$, though BC_{CMAQ} tends to overestimate BC between 1 km and 3 km. Figure 7b compares CMAQ modeled and observed total aerosol mass (SNA + OC + BC) averaged during the campaign. CMAQ modeled aerosol mass is on average biased low below 2 km, and biased high at higher altitudes (Fig. 7b).

Next, we evaluate how the vertical distribution of aerosols relates to extinction. Figure 7c compares the modeled and observed average vertical extinction profiles. We find, consistent with the biases in mass, a low bias in the modeled extinction profile below 2 km, and high bias above (Fig. 7c). The biases in extinction and the biases in mass have the same signs for more than 80% of data pairs, are strongly correlated (R = 0.85). This suggests that the aerosol vertical profile of extinction is mainly indicative of mass distribution. However, column AOD measures the vertical integral of light extinction by aerosols, which means the modeled AOD biases would be proportional to modeled surface $PM_{2.5}$ biases only if the biases in extinction are constant across all vertical layers. Since the biases of extinction change sign at higher altitude, the AOD biases reflect the competing effects of negative biases near the surface and positive biases at high altitudes, which lead to an overall negative bias of $PM_{2.5}$/AOD relationship, consistent with the negative NMB of $PM_{2.5}$/AOD in July shown in Fig. 4.

To explore the causes of the model-observation discrepancy in extinction and the resulting impacts on the satellite-derived surface $PM_{2.5}$, we calculate the vertical extinction profile in CMAQ by replacing the modeled aerosol mass distribution (SNA, OC, BC), or total mass extinction efficiency (MEE, total aerosol mass/extinction), or RH respectively with those of the aircraft observations, as shown in Fig. 8a. Replacing the modeled aerosol mass with observations, we find a decrease in extinction at high altitudes (above 2.5 km) and increase at low altitudes (below 2.5 km), but replacing the aerosol mass alone does not explain all of the model-observation differences. At high altitudes, only replacing the modeled total mass extinction efficiency without changing the mass captures the observed extinction. We attribute the model overestimate of extinction to model overestimation of extinction efficiency at high altitudes. A major contributor to the model overestimate of total MEE is its excessive RH at high altitudes, which leads to an overestimate of the hygroscopic growth. Replacing RH with observations largely corrects the high biases aloft, but does not correct the low biases below 2 km remain (Fig. 8a). At lower altitudes, the model low biases are due to model underestimates of both aerosol mass and total MEE. Model underestimates of MEE are likely due to: 1) uncertain optical properties; 2) other aerosols or gases (e.g. NO_2, O_3) or liquid clouds that can scatter or absorb light.

Figure 8b shows the biases of $PM_{2.5\_MAIAC}$ due to model uncertainties in vertical profiles of aerosol mass or MEE or RH, estimated by calculating the changes in $PM_{2.5}$ when we replace the model vertical profiles with observations. Since the aircraft altitude ranges from 0.3 to 3.4 km, we use modeled values for the layers below 0.3 km and above 3.4 km while attempting to minimize the discontinuity at both boundaries through vertical interpolation. As SNA and OC contribute most to extinction, we also evaluate the biases of vertical profiles of SNA and OC separately. We find that replacing modeled aerosol mass with observed mass leads to small positive biases in

$PM_{2.5\_MAIAC}$ (MB = 0.05 µg/m^3, SD = 4.3 µg/m^3), due to the combined effects of negative biases

from SNA (MB = -2.5 µg/m^3, SD = 4.7 µg/m^3) and positive biases from OC (MB = +1.9 µg/m^3,

SD = 4.3 µg/m^3).

We further separate the model-observation discrepancy in the vertical profiles as

differences in total column mass versus in vertical profile shape by 1) keeping the modeled vertical

distribution but adjusting the mass of each species uniformly so that the total column mass is equal

to observation; 2) keeping the total column mass the same as in the model but redistributing the

aerosol based on the observed vertical profiles. We find that redistributing the aerosol vertical

profile leads to a positive mean bias in $PM_{2.5\_MAIAC}$ (MB = 1.1 µg/m^3, SD = 4.9 µg/m^3), while the

model-observation discrepancy in column mass leads to a negative mean bias (MB = -0.6 µg/m^3,

SD = 3.6 µg/m^3) (Fig. 8b). The positive biases in the profile shape are mainly attributed to model

biases of the vertical profile of SNA (MB = 1.2 µg/m^3, SD = 5.0 µg/m^3), which shows a larger

fraction of SNA at higher altitude where aerosol is less effective at scattering light due to lower

RH. The negative MB of column mass reflects a combination of negative biases of SNA (MB = -

4.1 µg/m^3, SD = 5.6 µg/m^3) due to model overestimates of SNA column mass, and positive bias

of OC (MB = 6.7 µg/m^3, SD = 4.4 µg/m^3) due to model underestimate of column mass of OC.

Model biases in mass extinction efficiency lead to a small positive MB of 0.6 µg/m^3.

Using the observed $PM_{2.5}$/AOD acquired from paired AQS-AERONET sites, we estimate

that model biases in modeled $PM_{2.5}$/AOD lead to a negative MB of -0.9 µg/m^3 with large day-to-

day variability (SD = 9.8 µg/m^3) during the DISCOVER-AQ campaign, reflecting the model biases

from different sources as discussed above. Next, we evaluate which factor drives the daily

variability in the modeled $PM_{2.5}$/AOD biases the most by evaluating R value between the estimated

biases in modeled $PM_{2.5}$/AOD versus that attributed to individual factors. We find model bias in

aerosol mass is the most deterministic factor for the biases in modeled $PM_{2.5}$/AOD (R = 0.82, Fig. 8c). Model biases in aerosol mass can be due to either biases in column mass or vertical profile shape. We find model biases in modeled $PM_{2.5}$/AOD are more dependent on the biases in aerosol column mass (R = 0.79), instead of vertical profile shape. Model biases in mass extinction efficiency show moderate correlation with model biases of $PM_{2.5}$/AOD (R = 0.56). While model uncertainties in RH lead to an overall negative bias (MB = -1.7 $\mu g/m^3$, SD = 7.4 $\mu g/m^3$) to $PM_{2.5\_MAIAC}$, they are negatively correlated with model biases of $PM_{2.5}$/AOD (R = -0.25).

3.5.3 RH

Figure 8 suggests model biases in RH contribute a negative bias to the derived $PM_{2.5\_MAIAC}$ during the DISCOVER-AQ aircraft campaign. Here we evaluate the impacts of modeled RH (RH_{CMAQ}) biases on derived $PM_{2.5}$ throughout the year using six atmospheric soundings over the Northeast USA. We only assess the impacts of RH on the optical properties (i.e. hygroscopic growth) of aerosols. Comparing RH_{CMAQ} with observed RH (RH_{obs}), RH_{CMAQ} is overall biased high with the largest biases in winter. To evaluate the resulting impacts on AOD_{CMAQ}, we re-calculate the extinction using observed ambient RH from the soundings instead of RH_{CMAQ} in Eq. (4). Replacing RH_{CMAQ} with RH_{obs} decreases extinction by ~50% on average from the surface to 5km in both JJA and DJF (black lines in Fig. 9a and b). As AOD is the vertical integral of extinction, the total area between EXT_{sonde} and EXT_{CMAQ} (gray shading in Fig. 9a and b) indicates the differences in AOD due to differences in RH. The differences in RH below 3km in DJF, MAM and SON contribute more than 80% to the total differences in AOD. In JJA, the contribution from higher versus lower altitudes is similar, despite small model RH biases below 2 km.

We evaluate how the model-observation discrepancy in RH affects the derived $PM_{2.5}$ by calculating the changes in $PM_{2.5\_MAIAC}$ ($\Delta PM_{2.5\_RH}$) if EXT_{sonde} is used instead of EXT_{CMAQ}. As

expected, model errors in RH lead to a negative bias in derived $PM_{2.5\_MAIAC}$ of 3 $\mu g/m^3$ on average

(Fig. 9c). The negative biases in $PM_{2.5\_MAIAC}$ due to RH are largest in spring (-3.5 $\mu g/m^3$), and

smallest in summer (-1.6 $\mu g/m^3$). The hygroscopic growth factor is nonlinearly correlated with RH,

which increases more rapidly at high RH (> 80%) than at low to median RH (<80%, Fig. S2).

5   Compared with median RH conditions, model RH errors lead to more than double $\Delta PM_{2.5\_RH}$ (-

6.4 $\mu g/m^3$ versus 3 $\mu g/m^3$) when observed near-surface RH > 80% (Fig. 9d). At RH > 95%, we

find that the $\Delta PM_{2.5\_RH}$ can be as large as -20 $\mu g/m^3$ (Fig. 9d). Despite the large impacts of model

errors of RH at humid conditions, there is no significant correlation between $\Delta PM_{2.5\_RH}$ and

$\Delta PM_{2.5\_MAIAC}$ (R = 0.18, evaluated at nearby sites within 10 km), suggesting that uncertainty in

10   RH is not a main contributor to the random uncertainties in satellite-derived $PM_{2.5}$.

3.5.4   Uncertainties in the parameterization of aerosol optical properties

In previous sections, we demonstrated that the satellite-derived $PM_{2.5}$ depends on the

accuracy of the model simulation. Even with a perfect simulation, satellite-derived $PM_{2.5}$ will be

sensitive to the parameterization of aerosol optical properties, which would affect the mass-

15   extinction efficiency. We evaluate the uncertainties associated with the parameterization of aerosol

optical properties by varying each parameter (Table 1), and calculate the corresponding changes

in the derived $PM_{2.5\_MAIAC}$. Figure 10 shows the range of uncertainty in annual average $PM_{2.5\_MAIAC}$

due to uncertain aerosol size distributions, hygroscopicity, refractive index and aerosol species

density.

20   The size of a particle is a defining characteristic of aerosol light extinction (Mishchenko et

al., 1999). To evaluate model sensitivities to the uncertainties in size distribution, we vary the r_0

of SNA from 0.05 to 0.15 with a 0.02 increase each time, to cover the range of values reported in

the literature. For OC, we calculate AOD_{CMAQ} with r_0 = 0.02, 0.06, 0.09 and 0.12 μm, all values

used in previous studies (Hess et al., 1998; Chin et al., 2002; Highwood, 2009; Drury et al., 2010). Annual average $PM_{2.5\_MAIAC}$ could vary by up to 5 µg/m^3 (32%) with the choice of modal radius of either r_{SNA} or r_{OC}, which is the largest source of uncertainty among the four parameters (Fig. 10). We find that AOD_{CMAQ} reaches a maximum with r_{SNA} = 0.07 µm (r_{eff} = 0.12 µm), and minimum with r_{SNA} = 0.05 (r_{eff} = 0.15 µm), while $PM_{2.5\_MAIAC}$ reaches a maximum with r_{SNA} = 0.05 (r_{eff} = 0.09 µm), and minimum with r_{SNA} = 0.11 (r_{eff} = 0.19 µm), suggesting the impacts of size distribution are nonlinear and non-uniform (Fig. S3). Mie scattering of a particle tends to be most effective when the particle's diameter is near the wavelength of interest (0.55 µm). As hygroscopic particle growth also affects the size distribution, depending on ambient RH and the hygroscopic growth factor, reducing (or increasing) the dry effective radius could either move the bulk aerosol size closer to or further from 0.55 µm, and thus either increase or decrease the extinction. For OC, as the effective radius and the hygroscopic growth factor are smaller than for SNA, increasing the modal radius leads to more effective scattering, thus larger AOD_{CMAQ} and smaller $PM_{2.5\_MAIAC}$. Relative to the default r_{OC} = 0.09 µm assumed by Drury et al. (2010), using the r_{OC} (0.02 µm) recommended by Chin et al. (2002a) increases $PM_{2.5\_MAIAC}$ by 5 µg/m^3 (32%) on average, worsening the positive biases of $PM_{2.5\_MAIAC}$. Increasing r_{OC} to 0.12 µm as recommended by Highwood et al. (2009) has little effect, decreasing $PM_{2.5\_MAIAC}$ by 2% on average.

The uncertainty of hygroscopicity lies in two aspects: (1) the function shape and (2) the parameters. Figure S2 compares the κ function shape with the hygroscopic growth factors used by the IMPROVE network (Hand and Malm, 2006), the default algorithm used to calculate AOD online in CMAQ, with that proposed by Chin et al. (2002) (Table 1). Using the DISCOVER-AQ aircraft data to evaluate the parameterization of hygroscopic growth, we find that the κ parameter

best characterizes the observed hygroscopic growth factor (Fig. S2c). Latimer and Martin (2018) similarly found that implementing a κ formulation instead of hygroscopic growth based on OPAC improved the GEOS-Chem representation of mass scattering efficiency. Thus, we choose the κ parameter to represent the hygroscopic growth factor, and the uncertainty estimate here only reflects uncertainties in the κ parameter. In practice changes in aerosol composition could have even larger effects on hygroscopicity than uncertainties in κ as discussed in Sect. 3.5.1.

To test the sensitivity of satellite derived $PM_{2.5}$ to uncertainties in the κ parameter, we compute AOD_{CMAQ} using the low (0.33) and high end of κ (0.72) for SNA as suggested by Koehler et al. (2006). As the hygroscopic properties of inorganic salts are relatively well-known, the range of uncertainty for f(RH) of SNA is 30% at most (Fig. S2b). OC, on the other hand, is composed of thousands of species with distinct hygroscopicities. Assuming $κ_{OC}$ ranges from 0 (non-hygroscopic) to 0.2 (Jimenez et al., 2009; Duplissy et al., 2011), the range of f(RH) of OC can be as large as a factor of 2 at high RH>96% (Fig. S2a). Despite the larger uncertainty of $κ_{oc}$, we find the overall impacts of the uncertainties of $κ_{oc}$ on the derived $PM_{2.5}$ (0.3 $μg/m^3$, 2% of annual average $PM_{2.5\_MAIAC}$) are smaller than that of $κ_{SNA}$ (1.6 $μg/m^3$, 11% of annual average $PM_{2.5\_MAIAC}$). The small impacts of $κ_{oc}$ reflect the relatively small portion and the less hygroscopic nature of OC. For single observations, varying $κ_{SNA}$ leads to a maximum increase in $PM_{2.5\_MAIAC}$ by 20% and a maximum decrease by 28%. Varying $κ_{oc}$ increases $PM_{2.5\_MAIAC}$ by 10% or decrease $PM_{2.5\_MAIAC}$ by 18% at most. The overall impact of the uncertainties of $κ_{SNA}$ ranks second among the four parameters for SNA, while $κ_{OC}$ has the smallest impacts on the derived $PM_{2.5}$ (Fig. 10).

The refractive index (m) determines the Mie extinction efficiency, which is subject to uncertainties mostly due to the lack of measurements (Kanakidou et al., 2005). m_{SNA} in OPAC (default value) is slightly different from that recommended in Chin et al. (2002) and Highwood

(2009). Moise et al. (2015) suggest m_{OC} varies by species, with its real part ranging from 1.37 to 1.65. We calculated another version of AOD_{CMAQ} by varying the real part of m_{SNA} and m_{OC} using the lowest and highest values reported in the literature. We find the annual average $PM_{2.5\_MAIAC}$ decreased by 0.8 μg/m³ (6%) using the high end of m_{R_SNA}, while increased by 1.3 μg/m³ (9%) on average using the low end. Though m_{R_OC} has a wider range of uncertainty, its impacts on $PM_{2.5\_MAIAC}$ (-4% to +6%) are smaller than that of m_{R_SNA}. While the overall impacts on $PM_{2.5\_MAIAC}$ due to uncertainties of m_{R_SNA} are generally within 10% for single observations, $PM_{2.5\_MAIAC}$ can change by more than 20% under SNA dominated and high RH environments. The overall uncertainty due to m_{R_OC} is generally within 5% for single observations, with a few cases (<10% of the total data) where the relative change in $PM_{2.5\_MAIAC}$ can exceed 10%.

As aerosol density (ρ) is assumed to be constant for each species, varying ρ has the same effect on the extinction of given species. We vary the aerosol density of SNA from 1.65 to 1.83 g/cm³ based on the uncertainty estimate from a laboratory study of Sarangi et al. (2016), which translates to an uncertainty of -3% to 7% for AOD_{SNA}, and the aerosol density of OC from 1.2 to 1.78 g/cm³ following Park et al. (2006), which translates to an uncertainty in AOD_{OC} ranging from -8% to 37%. We find aerosol species density, in general, contributes least to the overall uncertainty in satellite-derived $PM_{2.5}$. Varying $ρ_{oc}$ across the range in Table 1 increases annual average $PM_{2.5\_MAIAC}$ by 0.9 μg/m³ (6%) or decreases it by 0.6 μg/m³ (3%) at most. As the aerosol density of inorganic salt is less uncertain, varying $ρ_{sulf}$ leads to negligible changes in annual average $PM_{2.5\_MAIAC}$ at both high (0.7 μg/m³, 5%) and low (-0.5 μg/m³, -2%) ends.

4   Conclusions

We derive surface $PM_{2.5}$ distributions from satellite observations of AOD (MAIAC products) at 1 km resolution for 2011 over the Northeast USA using a geophysical approach that

simulates the relationship between surface $PM_{2.5}$ and AOD with a regional air quality model (CMAQ) and offline AOD calculation package (FlexAOD). We find that the fine spatial resolution of MAIAC AOD reveals more spatial detail ("hot spots") including over populated urban areas or along major roadways. While the geophysical approach has shown promise for mapping the $PM_{2.5}$

5   exposure at seasonal to annual scales (van Donkelaar et al., 2010; 2016), we show that estimating $PM_{2.5}$ from satellite AOD at the daily scale is not only subject to large measurement uncertainty in satellite AOD products, but more importantly, to uncertainty in daily variations of the relationship between surface $PM_{2.5}$ and column AOD. We take advantage of multi-platform *in situ* observations available over the Northeast USA to quantify different sources of uncertainties in the satellite-

10   derived $PM_{2.5}$, with a particular focus on the daily scale. We use observed AOD from AERONET sun photometers to quantify uncertainties in satellite and modeled AOD; co-located AQS $PM_{2.5}$ and AERONET sites to evaluate modeled $PM_{2.5}$/AOD relationships; IMPROVE and CSN aerosol speciation data to evaluate model uncertainties of aerosol composition; atmospheric soundings to evaluate modeled RH, as well as their impacts on $PM_{2.5}$ derivation. To assess the uncertainties

15   associated with aerosol vertical profiles, we use the extensive concurrent measurements of extinction and aerosol composition available from the NASA DISCOVER-AQ 2011 campaign over Baltimore-Washington, D.C. Finally, we estimate intrinsic uncertainties associated with the model parameterization of optical properties, by testing sensitivities of satellite-derived $PM_{2.5}$ to variations in each individual parameter across ranges reported in the literature using FlexAOD.

20   As the relationship between surface $PM_{2.5}$ and column AOD is non-linear and spatiotemporally heterogeneous, satellite AOD alone is unable to fully resolve the spatial and temporal variability of ground-level $PM_{2.5}$. We find that large-scale spatial and temporal variability of satellite-derived $PM_{2.5}$ correlates more strongly with the variability in modeled $PM_{2.5}$/AOD than

with satellite derived AOD. At the daily scale over the Northeast USA, modeled $PM_{2.5}$/AOD introduce larger mean biases to satellite-derived $PM_{2.5}$ than the satellite retrievals. Uncertainties in modeled $PM_{2.5}$/AOD explain more than 70% variance in the uncertainties of satellite-derived $PM_{2.5}$, suggesting that the precision of daily satellite-derived $PM_{2.5}$ depends on the capability of

5   models to simulate the day-to-day variability of the relationship between $PM_{2.5}$ and AOD.

Uncertainties in modeled $PM_{2.5}$/AOD relationships can be attributed to several factors, including uncertain model aerosol speciation, vertical profiles, RH, and the parameterization of aerosol optical properties. We find that seasonally varying biases in modeled $PM_{2.5}$/AOD reflect biases in aerosol speciation, particularly OC, which is overestimated in the cold season, and

10   underestimated by CMAQ in the warm season. Biases in aerosol composition in turn affect aerosol hygroscopicity. The CMAQ model generally overestimates RH, especially above 2 km, contributing to an overall negative bias to satellite-derived $PM_{2.5}$, particularly for more humid conditions. Using concurrent measurements of vertical profiles of aerosol extinction and composition available from the DISCOVER-AQ 2011 aircraft campaign, we show that the aerosol

15   extinction is indicative of mass distributions. Biases in modeled extinction, however, vary with altitude, such that model biases in vertically integrated column AOD do not necessarily reflect model biases in surface $PM_{2.5}$. We find that model uncertainties in column mass and in the mass-extinction efficiency drive the variability in overall uncertainty in modeled $PM_{2.5}$/AOD, while RH and aerosol vertical profile shape contribute some systematic bias.

20   Even with a model that perfectly simulates the distribution of aerosols, calculating AOD is subject to additional uncertainties in aerosol size distributions, hygroscopic growth factors refractive indices and aerosol density. Our uncertainty analysis involving a series of sensitivity tests in FlexAOD indicates that for SNA, the uncertainties in size distributions contribute most to

uncertainty in the derived $PM_{2.5}$ (32%), followed by the hygroscopicity parameter κ (11%), refractive index (9%), and aerosol density (5%). For OC, size distribution is also the largest source of uncertainty in the derived $PM_{2.5}$ (32%). Despite the large uncertainty of the hygroscopicity of OC, its impact on the satellite-derived $PM_{2.5}$ is negligible (2%), even smaller than uncertainties associated with the refractive index and aerosol density (6% each).

Based on this uncertainty analysis, we identify opportunities and directions to develop the applications of satellite-derived $PM_{2.5}$ using the geophysical approach, especially at finer spatial and temporal scales. Van Donkelaar et al. (2016) found that calibration with ground-based $PM_{2.5}$ measurements improves the performance of satellite-based $PM_{2.5}$ at the annual scale, although such calibration is more challenging at short time scales (van Donkelaar et al., 2012). As the uncertainties in satellite-derived $PM_{2.5}$ reflect multiple factors, calibration targeting specific sources of uncertainty would help further refine the geophysical approach. Additional collocated measurements of both $PM_{2.5}$ and AOD would be valuable to further evaluate the relationship between surface $PM_{2.5}$ and satellite AOD (Snider et al. 2015). Routine measurements of aerosol vertical profiles would aid uncertainty attribution and likely lead to improved models and thereby reduce the overall uncertainty in satellite-derived $PM_{2.5}$. Quantifying source-specific uncertainties would not only facilitate future model improvement, but more importantly, benefit applications of the satellite-derived $PM_{2.5}$ products to health studies.

Author contribution: XJ, AF, AD, and RM designed the experiments. GC developed the FlexAOD code for CMAQ. AL provided MAIAC AOD data. KC and MK conducted the CMAQ simulation. XJ carried out the data analysis and prepared the manuscript with contributions from all co-authors.

5   **Data availability:** The CMAQ model output can be obtained by contacting Xiaomeng Jin (xjin@ldeo.columbia.edu). The FlexAOD code is available upon request by contacting Gabriele Curci (gabriele.curci@aquila.infn.it).

Competing interests: The authors declare that they have no conflict of interest.

Acknowledgement: Support for this study was provided by New York State Energy Research and

10   Development Authority (Grant number: 91268) and NASA Health and Air Quality Applied Sciences Team (HAQAST, Grant NNX16AQ20G). The authors thank Melanie Follette-Cook of NASA GSFC and Morgan State University for her help in obtaining the DISCOVER-AQ aircraft data. The authors thank Gus Correa for his help in obtaining, processing and archiving CMAQ data. We acknowledge useful discussions with Yang Liu from Emory University and Dan

15   Westervelt from Lamont-Doherty Earth Observatory of Columbia University.

Disclaimer: Although this manuscript was reviewed internally, it does not necessarily reflect the views or policies of the New York State Department of Environmental Conservation.

References

Adams, P. J.: Predicting global aerosol size distributions in general circulation models, J. Geophys. Res., 107(D19), 13,791–AAC 4–23, doi:10.1029/2001JD001010, 2002.

Appel, K. W., Pouliot, G. A., Simon, H., Sarwar, G., Pye, H. O. T., Napelenok, S. L., Akhtar, F. and Roselle, S. J.: Evaluation of dust and trace metal estimates from the Community Multiscale Air Quality (CMAQ) model version 5.0, Geosci. Model Dev., 6(4), 883–899, doi:10.5194/gmd-6-883-2013, 2013.

Appel, K. W., Napelenok, S. L., Foley, K. M., Pye, H. O. T., Hogrefe, C., Luecken, D. J., Bash, J. O., Roselle, S. J., Pleim, J. E., Foroutan, H., Hutzell, W. T., Pouliot, G. A., Sarwar, G., Fahey, K. M., Gantt, B., Gilliam, R. C., Heath, N. K., Kang, D., Mathur, R., Schwede, D. B., Spero, T. L., Wong, D. C. and Young, J. O.: Description and evaluation of the Community Multiscale Air Quality (CMAQ) modeling system version 5.1, Geosci. Model Dev., 10(4), 1703–1732, doi:10.5194/gmd-10-1703-2017, 2017.

Bey, I., Jacob, D. J., Yantosca, R. M., Logan, J. A., Field, B. D., Fiore, A. M., Li, Q. B., Liu, H., Mickley, L. J. and Schultz, M. G.: Global modeling of tropospheric chemistry with assimilated meteorology: Model description and evaluation, J. Geophys. Res. Atmos., 106(D19), 23073–23095, doi:10.1029/2001JD000807, 2001.

Brock, C. A., Wagner, N. L., Anderson, B. E., Attwood, A. R., Beyersdorf, A., Campuzano-Jost, P., Carlton, A. G., Day, D. A., Diskin, G. S., Gordon, T. D., Jimenez, J. L., Lack, D. A., Liao, J., Markovic, M. Z., Middlebrook, A. M., Ng, N. L., Perring, A. E., Richardson, M. S., Schwarz, J. P., Washenfelder, R. A., Welti, A., Xu, L., Ziemba, L. D., and Murphy, D. M.: Aerosol optical properties in the southeastern United States in summer – Part 1: Hygroscopic growth, Atmos. Chem. Phys., 16, 4987-5007, https://doi.org/10.5194/acp-16-4987-2016, 2016.

Burnett, R., Chen, H., Szyszkowicz, M., Fann, N., Hubbell, B., Pope, C. A., Apte, J. S., Brauer, M., Cohen, A., Weichenthal, S., Coggins, J., Di, Q., Brunekreef, B., Frostad, J., Lim, S. S., Kan, H., Walker, K. D., Thurston, G. D., Hayes, R. B., Lim, C. C., Turner, M. C., Jerrett, M., Krewski, D., Gapstur, S. M., Diver, W. R., Ostro, B., Goldberg, D., Crouse, D. L., Martin, R. V., Peters, P., Pinault, L., Tjepkema, M., van Donkelaar, A., Villeneuve, P. J., Miller, A. B., Yin, P., Zhou, M., Wang, L., Janssen, N. A. H., Marra, M., Atkinson, R. W., Tsang, H., Quoc Thach, T., Cannon, J. B., Allen, R. T., Hart, J. E., Laden, F., Cesaroni, G.,

Forastiere, F., Weinmayr, G., Jaensch, A., Nagel, G., Concin, H. and Spadaro, J. V.: Global estimates of mortality associated with long-term exposure to outdoor fine particulate matter, Proc. Natl. Acad. Sci. U.S.A., 115(38), 9592–9597, doi:10.1073/pnas.1803222115, 2018.

Chin, M., Ginoux, P., Kinne, S., Torres, O., Holben, B. N., Duncan, B. N., Martin, R. V., Logan, J. A., Higurashi, A. and Nakajima, T.: Tropospheric aerosol optical thickness from the GOCART model and comparisons with satellite and Sun photometer measurements, Journal of the Atmospheric Sciences, 59(3), 461–483, doi:10.1175/1520-0469(2002)059<0461:TAOTFT>2.0.CO;2, 2002.

Cohen, A. J., Brauer, M., Burnett, R., Anderson, H. R., Frostad, J., Estep, K., Balakrishnan, K., Brunekreef, B., Dandona, L., Dandona, R., Feigin, V., Freedman, G., Hubbell, B., Jobling, A., Kan, H., Knibbs, L., Liu, Y., Martin, R., Morawska, L., Pope, C. A., III, Shin, H., Straif, K., Shaddick, G., Thomas, M., Van Dingenen, R., van Donkelaar, A., Vos, T., Murray, C. J. L. and Forouzanfar, M. H.: Estimates and 25-year trends of the global burden of disease attributable to ambient air pollution: an analysis of data from the Global Burden of Diseases Study 2015, The Lancet, 389(10082), 1907–1918, doi:10.1016/S0140-6736(17)30505-6, 2017.

Crouse, D. L. et al., Risk of Nonaccidental and Cardiovascular Mortality in Relation to Long-term Exposure to Low Concentrations of Fine Particulate Matter: A Canadian National-Level Cohort Study, Environmental Health Perspectives, 120(5), 708–714, doi:10.1289/ehp.1104049, 2012.

Crumeyrolle, S., Chen, G., Ziemba, L., Beyersdorf, A., Thornhill, L., Winstead, E., Moore, R. H., Shook, M. A., Hudgins, C. and Anderson, B. E.: Factors that influence surface $PM_{2.5}$ values inferred from satellite observations: perspective gained for the US Baltimore–Washington metropolitan area during DISCOVER-AQ, Atmos. Chem. Phys., 14(4), 2139–2153, doi:10.5194/acp-14-2139-2014, 2014.

Curci, G., Hogrefe, C., Bianconi, R., Im, U., Balzarini, A., Baró, R., Brunner, D., Forkel, R., Giordano, L., Hirtl, M., Honzak, L., Jiménez-Guerrero, P., Knote, C., Langer, M., Makar, P. A., Pirovano, G., Pérez, J. L., José, R. S., Syrakov, D., Tuccella, P., Werhahn, J., Wolke, R., Žabkar, R., Zhang, J. and Galmarini, S.: Uncertainties of simulated aerosol optical properties induced by assumptions on aerosol physical and chemical properties: An

AQMEII-2 perspective, Atmospheric Environment, 115(c), 541–552, doi:10.1016/j.atmosenv.2014.09.009, 2015.

de Hoogh, K., Gulliver, J., Donkelaar, A. V., Martin, R. V., Marshall, J. D., Bechle, M. J., Cesaroni, G., Pradas, M. C., Dedele, A., Eeftens, M., Forsberg, B., Galassi, C., Heinrich, J., Hoffmann, B., Jacquemin, B., Katsouyanni, K., Korek, M., Künzli, N., Lindley, S. J., Lepeule, J., Meleux, F., de Nazelle, A., Nieuwenhuijsen, M., Nystad, W., Raaschou-Nielsen, O., Peters, A., Peuch, V.-H., Rouil, L., Udvardy, O., Slama, R., Stempfelet, M., Stephanou, E. G., Tsai, M. Y., Yli-Tuomi, T., Weinmayr, G., Brunekreef, B., Vienneau, D. and Hoek, G.: Development of West-European PM2.5 and NO2 land use regression models incorporating satellite-derived and chemical transport modelling data, Environmental Research, 151, 1–10, doi:10.1016/j.envres.2016.07.005, 2016.

Di, Q., Kloog, I., Koutrakis, P., Lyapustin, A., Wang, Y. and Schwartz, J.: Assessing PM2.5 Exposures with High Spatiotemporal Resolution across the Continental United States, Environ. Sci. Technol., 50(9), 4712–4721, doi:10.1021/acs.est.5b06121, 2016.

Dockery, D. W., C. A. Pope, X. Xu, J. D. Spengler, J. H. Ware, M. E. Fay, B. G. Ferris Jr., and F. E. Speizer, An Association between Air Pollution and Mortality in Six U.S. Cities, N Engl J Med, *329*(24), 1753–1759, doi:10.1056/NEJM199312093292401, 1993.

Dominici, F., Peng, R. D., Bell, M. L., Pham, L., McDermott, A., Zeger, S. L. and Samet, J. M.: Fine Particulate Air Pollution and Hospital Admission for Cardiovascular and Respiratory Diseases, JAMA, 295(10), 1127–1134, doi:10.1001/jama.295.10.1127, 2006.

Drury, E., Jacob, D. J., Spurr, R. J. D., Wang, J., Shinozuka, Y., Anderson, B. E., Clarke, A. D., Dibb, J., McNaughton, C. and Weber, R.: Synthesis of satellite (MODIS), aircraft (ICARTT), and surface (IMPROVE, EPA-AQS, AERONET) aerosol observations over eastern North America to improve MODIS aerosol retrievals and constrain surface aerosol concentrations and sources, Journal of Geophysical Research: Atmospheres (1984–2012), 115(D14), D14204, doi:10.1029/2009JD012629, 2010.

Duplissy, J., DeCarlo, P. F., Dommen, J., Alfarra, M. R., Metzger, A., Barmpadimos, I., Prevot, A. S. H., Weingartner, E., Tritscher, T., Gysel, M., Aiken, A. C., Jimenez, J. L., Canagaratna, M. R., Worsnop, D. R., Collins, D. R., Tomlinson, J. and Baltensperger, U.: Relating hygroscopicity and composition of organic aerosol particulate matter, Atmos. Chem. Phys., 11(3), 1155–1165, doi:10.5194/acp-11-1155-2011, 2011.

Durre, I., and X. Yin, Enhanced Radiosonde Data for Studies of Vertical Structure, Bull. Amer. Meteor. Soc., *89*(9), 1257–1262, 2008. Retrieved from http://www.jstor.org/stable/26220887, last access: 8 December, 2018.

Ford, B. and Heald, C. L.: Aerosol loading in the Southeastern United States: reconciling surface and satellite observations, Atmos. Chem. Phys., 13(18), 9269–9283, doi:10.5194/acp-13-9269-2013, 2013.

Ford, B. and Heald, C. L.: Exploring the uncertainty associated with satellite-based estimates of premature mortality due to exposure to fine particulate matter, Atmos. Chem. Phys., 16(5), 3499–3523, doi:10.5194/acp-16-3499-2016, 2016.

Green, M., Kondragunta, S., Ciren, P. and Xu, C.: Comparison of GOES and MODIS Aerosol Optical Depth (AOD) to Aerosol Robotic Network (AERONET) AOD and IMPROVE PM 2.5Mass at Bondville, Illinois, Journal of the Air & Waste Management Association, 59(9), 1082–1091, doi:10.3155/1047-3289.59.9.1082, 2012.

Griffin, D., Naumova, E., McEntee, J., Castronovo, D., Durant, J., Lyles, M., Faruque, F. and Lary, D.: Air quality and human health, in Environmental Tracking for Public Health Surveillance, pp. 129–185, CRC Press. 2012.

Gupta, P. and Christopher, S. A.: Particulate matter air quality assessment using integrated surface, satellite, and meteorological products: Multiple regression approach, J. Geophys. Res., 114(D14), 1249–13, doi:10.1029/2008JD011496, 2009.

Hand, J. and Malm, W. C. Review of the IMPROVE equation for estimating ambient light extinction coefficients, Colorado State University, Fort Colins, 2006.

Hess, M., Koepke, P. and Schult, I.: Optical Properties of Aerosols and Clouds: The Software Package OPAC, Bull. Amer. Meteor. Soc., 79(5), 831–844, doi:10.1175/1520-0477(1998)079<0831:OPOAAC>2.0.CO;2, 1998.

Highwood, E.J., 5 August 2009. Suggested Refractive Indices and Aerosol Size Pa- rameters for Use in Radiative Effect Calculations and Satellite Retrievals. ADIENT/APPRAISE CP2 Technical Report, DRAFT V2. Retrieved from: http://www. reading.ac.uk/adient/refractiveindices.html, last access: 8 December, 2018.

Holben, B. N., Eck, T. F., Slutsker, I., Tanre, D., Buis, J. P., Setzer, A., Vermote, E., Reagan, J. A., Kaufman, Y. J., Nakajima, T., Lavenu, F., Jankowiak, I. and Smirnov, A.: AERONET - A

federated instrument network and data archive for aerosol characterization, Remote
Sensing of Environment, 66(1), 1–16, doi:10.1016/S0034-4257(98)00031-5, 1998.

Houyoux, M. R., Vukovich, J. M., Coats, C. J., Jr., Wheeler, N. J. M. and Kasibhatla, P. S.:
Emission inventory development and processing for the Seasonal Model for Regional Air
Quality (SMRAQ) project, J. Geophys. Res., 105(D7), 9079–9090,
doi:10.1029/1999JD900975, 2000.

Hu, X., Waller, L. A., Lyapustin, A., Wang, Y. and Liu, Y.: 10-year spatial and temporal trends of
$PM_{2.5}$ concentrations in the southeastern US estimated using high-resolution satellite data,
Atmos. Chem. Phys., 14(12), 6301–6314, doi:10.5194/acp-14-6301-2014, 2014.

Jerrett, M., Turner, M. C., Beckerman, B. S., Pope, C. A., van Donkelaar, A., Martin, R. V., Serre,
M., Crouse, D., Gapstur, S. M., Krewski, D., Diver, W. R., Coogan, P. F., Thurston, G. D.
and Burnett, R. T.: Comparing the Health Effects of Ambient Particulate Matter Estimated
Using Ground-Based versus Remote Sensing Exposure Estimates, EHP, 125(4), 1–8,
doi:10.1289/EHP575, 2017.

Jimenez, J. L., Canagaratna, M. R., Donahue, N. M., Prevot, A. S. H., Zhang, Q., Kroll, J. H.,
DeCarlo, P. F., Allan, J. D., Coe, H., Ng, N. L., Aiken, A. C., Docherty, K. S., Ulbrich, I.
M., Grieshop, A. P., Robinson, A. L., Duplissy, J., Smith, J. D., Wilson, K. R., Lanz, V. A.,
Hueglin, C., Sun, Y. L., Tian, J., Laaksonen, A., Raatikainen, T., Rautiainen, J., Vaattovaara,
P., Ehn, M., Kulmala, M., Tomlinson, J. M., Collins, D. R., Cubison, M. J., E., Dunlea, J.,
Huffman, J. A., Onasch, T. B., Alfarra, M. R., Williams, P. I., Bower, K., Kondo, Y.,
Schneider, J., Drewnick, F., Borrmann, S., Weimer, S., Demerjian, K., Salcedo, D., Cottrell,
L., Griffin, R., Takami, A., Miyoshi, T., Hatakeyama, S., Shimono, A., Sun, J. Y., Zhang,
Y. M., Dzepina, K., Kimmel, J. R., Sueper, D., Jayne, J. T., Herndon, S. C., Trimborn, A.
M., Williams, L. R., Wood, E. C., Middlebrook, A. M., Kolb, C. E., Baltensperger, U. and
Worsnop, D. R.: Evolution of Organic Aerosols in the Atmosphere, Science, 326(5959),
1525–1529, doi:10.1126/science.1180353, 2009.

Kanakidou, M., Seinfeld, J. H., Pandis, S. N., Barnes, I., Dentener, F. J., Facchini, M. C., Van
Dingenen, R., Ervens, B., Nenes, A., Nielsen, C. J., Swietlicki, E., Putaud, J. P., Balkanski,
Y., Fuzzi, S., Horth, J., Moortgat, G. K., Winterhalter, R., Myhre, C. E. L., Tsigaridis, K.,
Vignati, E., Stephanou, E. G., and Wilson, J.: Organic aerosol and global climate

modelling: a review, Atmos. Chem. Phys., 5, 1053-1123, https://doi.org/10.5194/acp-5-1053-2005, 2005.

Kim, P. S., Jacob, D. J., Fisher, J. A., Travis, K., Yu, K., Zhu, L., Yantosca, R. M., Sulprizio, M. P., Jimenez, J. L., Campuzano-Jost, P., Froyd, K. D., Liao, J., Hair, J. W., Fenn, M. A., Butler, C. F., Wagner, N. L., Gordon, T. D., Welti, A., Wennberg, P. O., Crounse, J. D., St Clair, J. M., Teng, A. P., Millet, D. B., Schwarz, J. P., Markovic, M. Z. and Perring, A. E.: Sources, seasonality, and trends of southeast US aerosol: an integrated analysis of surface, aircraft, and satellite observations with the GEOS-Chem chemical transport model, Atmos. Chem. Phys., 15(18), 10411–10433, doi:10.5194/acp-15-10411-2015, 2015.

Kloog, I., Chudnovsky, A. A., Just, A. C., Nordio, F., Koutrakis, P., Coull, B. A., Lyapustin, A., Wang, Y. and Schwartz, J.: A new hybrid spatio-temporal model for estimating daily multi-year PM2.5 concentrations across northeastern USA using high resolution aerosol optical depth data, Atmospheric Environment, 95, 581–590, doi:10.1016/j.atmosenv.2014.07.014, 2014.

Koehler, K. A., Kreidenweis, S. M., DeMott, P. J., Prenni, A. J., Carrico, C. M., Ervens, B., and Feingold, G.: Water activity and activation diameters from hygroscopicity data - Part II: Application to organic species, Atmos. Chem. Phys., 6, 795-809, https://doi.org/10.5194/acp-6-795-2006, 2006.

Laden, F., Schwartz, J., Speizer, F. E. and Dockery, D. W.: Reduction in Fine Particulate Air Pollution and Mortality, Am J Respir Crit Care Med, 173(6), 667–672, doi:10.1164/rccm.200503-443OC, 2006.

Latimer, R. N. C., and R. V. Martin, Interpretation of Measured Aerosol Mass Scattering Efficiency Over North America Using a Chemical Transport Model, Atmos. Chem. Phys. Discuss., *2018*, doi:10.5194/acp-2018-459, 2018.

Lee, H. J., Chatfield, R. B. and Strawa, A. W.: Enhancing the Applicability of Satellite Remote Sensing for PM2.5 Estimation Using MODIS Deep Blue AOD and Land Use Regression in California, United States, Environ. Sci. Technol., *50* (12), 6546-6555, doi:10.1021/acs.est.6b01438, 2016.

Levy, R. C., S. Mattoo, V. Sawyer, Y. Shi, P. R. Colarco, A. I. Lyapustin, Y. Wang, and L. A. Remer, Exploring systematic offsets between aerosol products from the two MODIS sensors, Atmos. Meas. Tech., *11*(7), 4073–4092, doi:10.5194/amt-11-4073-2018, 2018.

Lyapustin, A., Martonchik, J., Wang, Y., Laszlo, I. and Korkin, S.: Multiangle implementation of atmospheric correction (MAIAC): 1. Radiative transfer basis and look-up tables, Journal of Geophysical Research: Atmospheres (1984–2012), 116(D3), D03210, doi:10.1029/2010JD014985, 2011.

Lyapustin, A. I., Wang, Y., Laszlo, I., Hilker, T., G Hall, F., Sellers, P. J., Tucker, C. J. and Korkin, S. V.: Multi-angle implementation of atmospheric correction for MODIS (MAIAC): 3. Atmospheric correction, Remote Sensing of Environment, 127, 385–393, 2012.

Lyapustin, A., Wang, Y., Korkin, S., and Huang, D.: MODIS Collection 6 MAIAC algorithm, Atmos. Meas. Tech., 11, 5741-5765, https://doi.org/10.5194/amt-11-5741-2018, 2018a.

Lyapustin, A., Wang, Y. MCD19A2 MODIS/Terra+Aqua Land Aerosol Optical Depth Daily L2G Global 1km SIN Grid V006 [Data set]. NASA EOSDIS Land Processes DAAC. doi: 10.5067/MODIS/MCD19A2.006, 2018b.

Ming, Y., Ramaswamy, V., Ginoux, P. A. and Horowitz, L. H.: Direct radiative forcing of anthropogenic organic aerosol, J. Geophys. Res., 110(D20), 1097–12, doi:10.1029/2004JD005573, 2005.

Mishchenko, M. I., J. M. Dlugach, E. G. Yanovitskij, and N. T. Zakharova, Bidirectional reflectance of flat, optically thick particulate layers: an efficient radiative transfer solution and applications to snow and soil surfaces, Journal of Quantitative Spectroscopy and Radiative Transfer, 63(2), 409–432, doi:https://doi.org/10.1016/S0022-4073(99)00028-X, 1999.

Moise, T., Flores, J. M. and Rudich, Y.: Optical Properties of Secondary Organic Aerosols and Their Changes by Chemical Processes, Chem. Rev., 115(10), 4400–4439, doi:10.1021/cr5005259, 2015.

Park, S.-K., Marmur, A., Kim, S. B., Tian, D., Hu, Y., McMurry, P. H. and Russell, A. G.: Evaluation of Fine Particle Number Concentrations in CMAQ, Aerosol Science and Technology, 40(11), 985–996, doi:10.1080/02786820600907353, 2006.

Peng, R. D., Bell, M. L., Geyh, A. S., McDermott, A., Zeger, S. L., Samet, J. M. and Dominici, F.: Emergency Admissions for Cardiovascular and Respiratory Diseases and the Chemical Composition of Fine Particle Air Pollution, EHP, 117(6), 957–963, 2009.

Petters, M. D. and Kreidenweis, S. M.: A single parameter representation of hygroscopic growth and cloud condensation nucleus activity, Atmos. Chem. Phys., 7(8), 1961–1971, doi:10.5194/acp-7-1961-2007, 2007.

Pierce, T., C. Geron, G. Pouliot, E. Kinnee, and J. Vukovich: Integration of the Biogenic Emissions Inventory System (BEIS3) into the Community Multiscale Air Quality (CMAQ) Modeling System, Proceedings of the AMS 4th Urban Environment Symposium, Norfolk, Virginia, 20-23 May, 2002.

Raffuse, S. M., Pryden, D. A., Sullivan, D. C., Larkin, N. K., Strand, T., &Solomon, R.: SMARTFIRE algorithm description. Paper prepared for the U.S. Environmental Protection Agency, Research Triangle Park, NC, by Sonoma Technology, Inc., Petaluma, CA, and the U.S. Forest Service, AirFire Team, Pacific Northwest Research Laboratory, Seattle, WA STI-905517-3719, October, 2009.

Sarangi, B., Aggarwal, S. G., Sinha, D. and Gupta, P. K.: Aerosol effective density measurement using scanning mobility particle sizer and quartz crystal microbalance with the estimation of involved uncertainty, Atmos. Meas. Tech., 9(3), 859–875, doi:10.5194/amt-9-859-2016, 2016.

Shaddick, G., Thomas, M. L., Green, A., Brauer, M., van Donkelaar, A., Burnett, R., Chang, H. H., Cohen, A., Dingenen, R. V., Dora, C., Gumy, S., Liu, Y., Martin, R., Waller, L. A., West, J., Zidek, J. V. and Prüss-Ustün, A.: Data integration model for air quality: a hierarchical approach to the global estimation of exposures to ambient air pollution, J. R. Stat. Soc. C, 67(1), 231–253, doi:10.1111/rssc.12227, 2017.

Shi, L., Zanobetti, A., Kloog, I., Coull, B. A., Koutrakis, P., Melly, S. J. and Schwartz, J. D.: Low-Concentration PM2.5 and Mortality: Estimating Acute and Chronic Effects in a Population-Based Study, EHP, 124(1), 1–30, doi:10.1289/ehp.1409111, 2015.

Snider, G. et al. (2015), SPARTAN: a global network to evaluate and enhance satellite-based estimates of ground-level particulate matter for global health applications, *Atmos. Meas. Tech.*, *8*(1), 505–521, doi:10.5194/amt-8-505-2015.

Snider, G., Weagle, C. L., Murdymootoo, K. K., Ring, A., Ritchie, Y., Stone, E., Walsh, A., Akoshile, C., Anh, N. X., Balasubramanian, R., Brook, J., Qonitan, F. D., Dong, J., Griffith, D., He, K., Holben, B. N., Kahn, R., Lagrosas, N., Lestari, P., Ma, Z., Misra, A., Norford, L. K., Quel, E. J., Salam, A., Schichtel, B., Segev, L., Tripathi, S., Wang, C., Yu, C., Zhang,

Q., Zhang, Y., Brauer, M., Cohen, A., Gibson, M. D., Liu, Y., Martins, J. V., Rudich, Y. and Martin, R. V.: Variation in global chemical composition of $PM_{2.5}$: emerging results from SPARTAN, Atmos. Chem. Phys., 16(15), 9629–9653, doi:10.5194/acp-16-9629-2016, 2016.

5   Stanier, C. O., Khlystov, A. Y. and Pandis, S. N.: Ambient aerosol size distributions and number concentrations measured during the Pittsburgh Air Quality Study (PAQS), Atmospheric Environment, 38(20), 3275–3284, doi:10.1016/j.atmosenv.2004.03.020, 2004.

Superczynski, S. D., Kondragunta, S. and Lyapustin, A. I.: Evaluation of the multi-angle implementation of atmospheric correction (MAIAC) aerosol algorithm through
10   intercomparison with VIIRS aerosol products and AERONET, J. Geophys. Res. Atmos., 122(5), 3005–3022, doi:10.1002/2016JD025720, 2017.

Toth, T. D., Zhang, J., Campbell, J. R., Hyer, E. J., Reid, J. S., Shi, Y. and Westphal, D. L.: Impact of data quality and surface-to-column representativeness on the $PM_{2.5}$/satellite AOD relationship for the contiguous United States, Atmos. Chem. Phys., 14(12), 6049–6062,
15   doi:10.5194/acp-14-6049-2014, 2014.

US EPA, MOVES2014a: Latest version of MOtor Vehicle Emission Simulator (MOVES): https://www.epa.gov/moves/moves2014a-latest-version-motor-vehicle-emission-simulator-moves, last accessed in April 2018.

van Donkelaar, A., Martin, R. V. and Park, R. J.: Estimating ground-level PM2.5 using aerosol
20   optical depth determined from satellite remote sensing, J. Geophys. Res., 111(D21), D21201−10, doi:10.1029/2005JD006996, 2006.

van Donkelaar, A., Martin, R. V., Brauer, M., Kahn, R., Levy, R., Verduzco, C. and Villeneuve, P. J.: Global Estimates of Ambient Fine Particulate Matter Concentrations from Satellite-Based Aerosol Optical Depth: Development and Application, EHP, 118(6), 847–855,
25   doi:10.1289/ehp.0901623, 2010.

van Donkelaar, A., Martin, R. V., Pasch, A. N., Szykman, J. J., Zhang, L., Wang, Y. X. and Chen, D.: Improving the Accuracy of Daily Satellite-Derived Ground-Level Fine Aerosol Concentration Estimates for North America, Environ. Sci. Technol., 46(21), 11971–11978, doi:10.1021/es3025319, 2012.

van Donkelaar, A., Martin, R. V., Spurr, R. J. D., Drury, E., Remer, L. A., Levy, R. C. and Wang, J.: Optimal estimation for global ground-level fine particulate matter concentrations, J. Geophys. Res. Atmos., 118(11), 5621–5636, doi:10.1002/jgrd.50479, 2013.

van Donkelaar, A., R. V. Martin, R. J. D. Spurr, and R. T. Burnett, High-Resolution Satellite-Derived $PM_{2.5}$ from Optimal Estimation and Geographically Weighted Regression over North America, Environ. Sci. Technol., *49*(17), 10482–10491, doi:10.1021/acs.est.5b02076, 2015.

van Donkelaar, A., Martin, R. V., Brauer, M., Hsu, N. C., Kahn, R. A., Levy, R. C., Lyapustin, A., Sayer, A. M. and Winker, D. M.: Global Estimates of Fine Particulate Matter using a Combined Geophysical-Statistical Method with Information from Satellites, Models, and Monitors, Environ. Sci. Technol., 50(7), 3762–3772, doi:10.1021/acs.est.5b05833, 2016.

Zhang, Y., Vijayaraghavan, K., Wen, X.-Y., Snell, H. E. and Jacobson, M. Z.: Probing into regional ozone and particulate matter pollution in the United States: 1. A 1 year CMAQ simulation and evaluation using surface and satellite data, J. Geophys. Res., 114(D22), D22304, doi:10.1029/2009JD011898, 2009.

Table 1: Optical properties used to calculate AOD_{CMAQ} in FlexAOD. Values in square brackets represent the range of uncertainties for each parameter, which we used for in FlexAOD sensitivity tests to quantify their impacts on the satellite-derived $PM_{2.5}$.

	Sulfate	OC	BC	Sea Salt	Dust
Modal radius [a] (r_0, μm)	0.11^b [0.05^c ~ 0.15]	0.09^b [0.02^d ~ 0.12^c]	0.02^b	0.40^b	
Geometric standard deviation [a] (σ_g)	1.6^b	1.6^b	1.6^b	1.5^b	
Aerosol density (ρ, g/cm^3)	1.7^b [1.65, 1.83]^e	1.3^b [1.2, 1.78]^f	1.0^b	2.2^b	
Refractive Index (m) at 550 nm	1.53^g [1.43^d, 1.6^c] $- i0.006^g$	1.53^g [1.37, $1.65]^h - i0.008$	$1.75 - i0.44^g$	$1.5 - i10^{-8\,g}$	$1.53 - i0.0055^g$
Hygroscopic growth factor (f) at RH = 90%	1.77 [1.58, 1.96]^i	1.24^j [1.0^k, 1.41^j]	1.4^d	2.4^d	1.0^d
	1.8^d	1.6^d	1.4^d	2.4^d	1.0^d
	5.1^k	1.0^k	1.4^d	2.4^d	1.0^d

Note:

    a. Assuming log-normal distributions for all aerosol species except for dust. The effective radius is calculated as: $r_e = r_0 e^{(\frac{5}{2}\ln^2 \sigma_g)}$.

    b. Drury et al. (2010).

10   c. Highwood et al. (2009).

    d. Chin et al. (2002)

    e. Sarangi et al., (2016)

    f. Park et al., (2006)

    g. OPAC (Hess et al., 1998)

15   h. Moise et al., (2015)

    i. κ parameter (Petters and Kreidenweis, 2007). The hygroscopic factor (f) is calculated as: $f(RH) = (1 + \kappa \frac{RH}{100\text{-}RH})^{1/3}$ following Snider et al. (2016), where κ = 0.53 in the default run, κ = 0.33 for the low end, κ = 0.72 for the high end.

    j. Calculated from κ parameter equation, where κ = 0.1 in the default run, κ = 0.2 for the high end
20   (Jimenez et al., 2009; Duplissy et al., 2011).

    k. Empirical hygroscopic growth factors used by the revised IMPROVE algorithm (Hand and Malm, 2006) to calculate light extinction (http://vista.cira.colostate.edu/Improve/the-improve-algorithm/). The revised IMPROVE algorithm assumes no hygroscopic growth for OC.
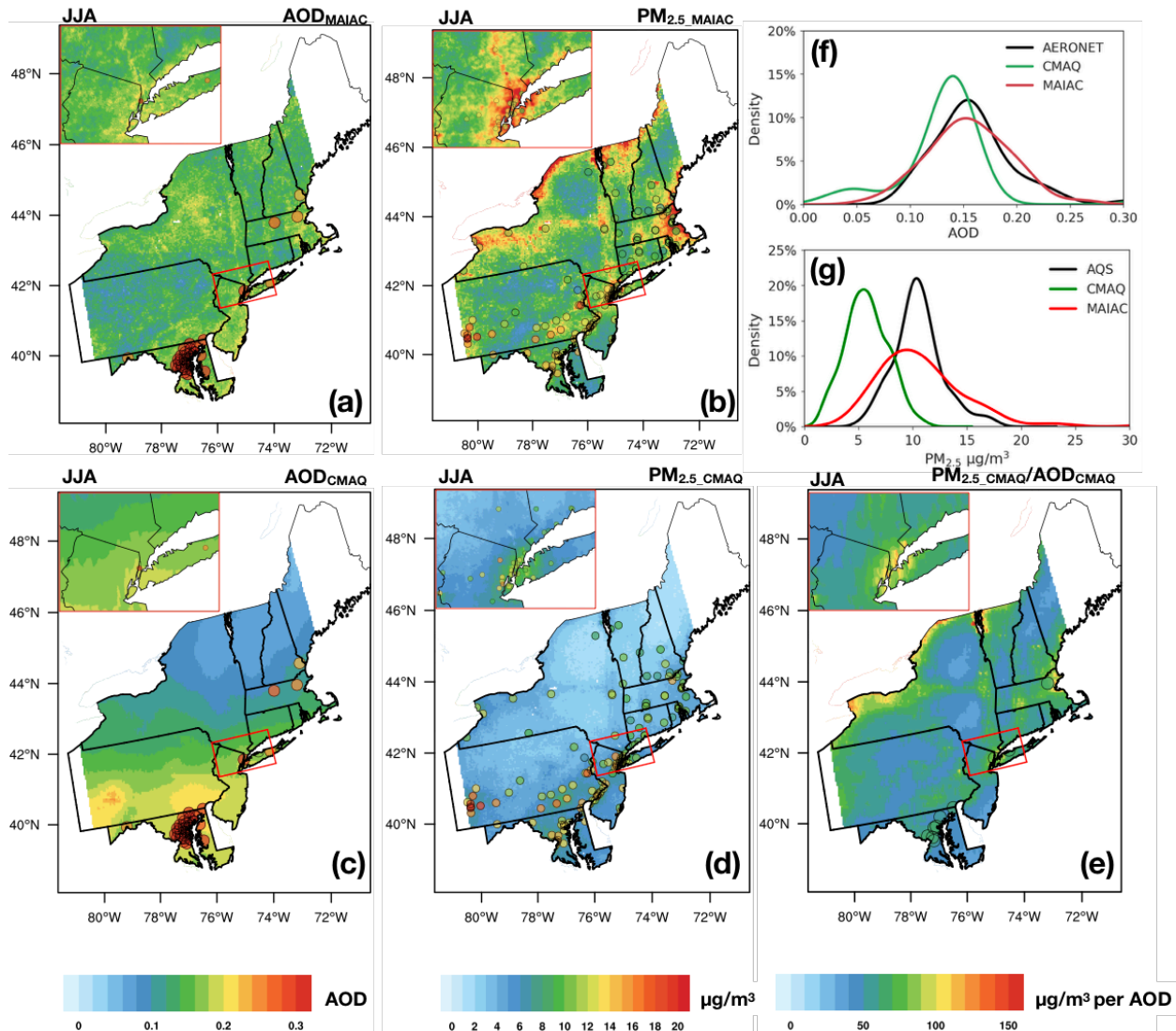
Figures

Figure 1 Summertime (JJA) average: (a) MAIAC AOD (AOD$_{MAIAC}$); (b) satellite-derived PM$_{2.5}$ (PM$_{2.5\_MAIAC}$); (c) CMAQ model AOD (AOD$_{CMAQ}$); (d) CMAQ model PM$_{2.5}$ (PM$_{2.5\_CMAQ}$); (e) CMAQ modeled PM$_{2.5}$/AOD (PM$_{2.5\_CMAQ}$/AOD$_{CMAQ}$) ratio overlaid with ground-based observations (AERONET, AQS, co-located AERONET and AQS sites) over the Northeast USA with zoom-in maps over the New York City region in the upper left corner. (f) Density plot of AOD showing the distribution of MAIAC, CMAQ and AERONET observed AOD sampled at AERONET sites. (g) Density plot of PM$_{2.5}$ showing the distribution of satellite-derived, CMAQ and AQS observed PM$_{2.5}$ sampled at AQS sites.
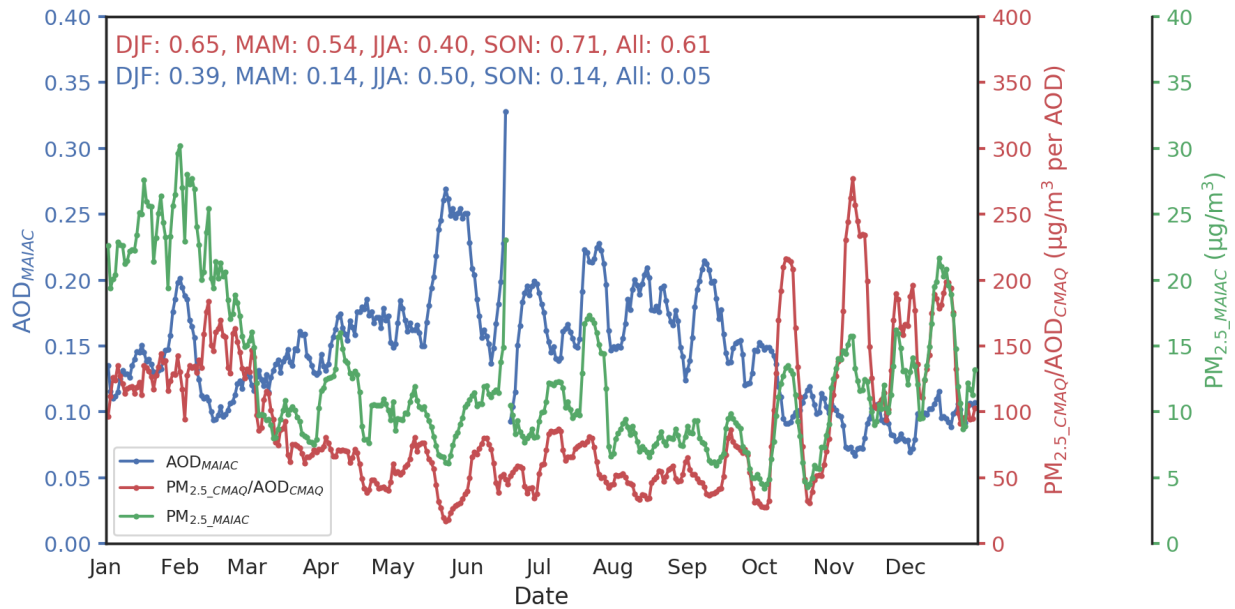
Figure 2 Regional 10-day running average of (a) MAIAC AOD (AOD_{MAIAC}, blue); (b) CMAQ modeled $PM_{2.5}$/AOD relationship ($PM_{2.5\_CMAQ}/AOD_{CMAQ}$, red); and (c) satellite derived $PM_{2.5}$ ($PM_{2.5\_MAIAC}$, green). The numbers on the upper left corner show the Pearson correlation coefficients (R) of $PM_{2.5\_MAIAC}$ with $PM_{2.5\_CMAQ}/AOD_{CMAQ}$ (red) and AOD_{MAIAC} (blue).
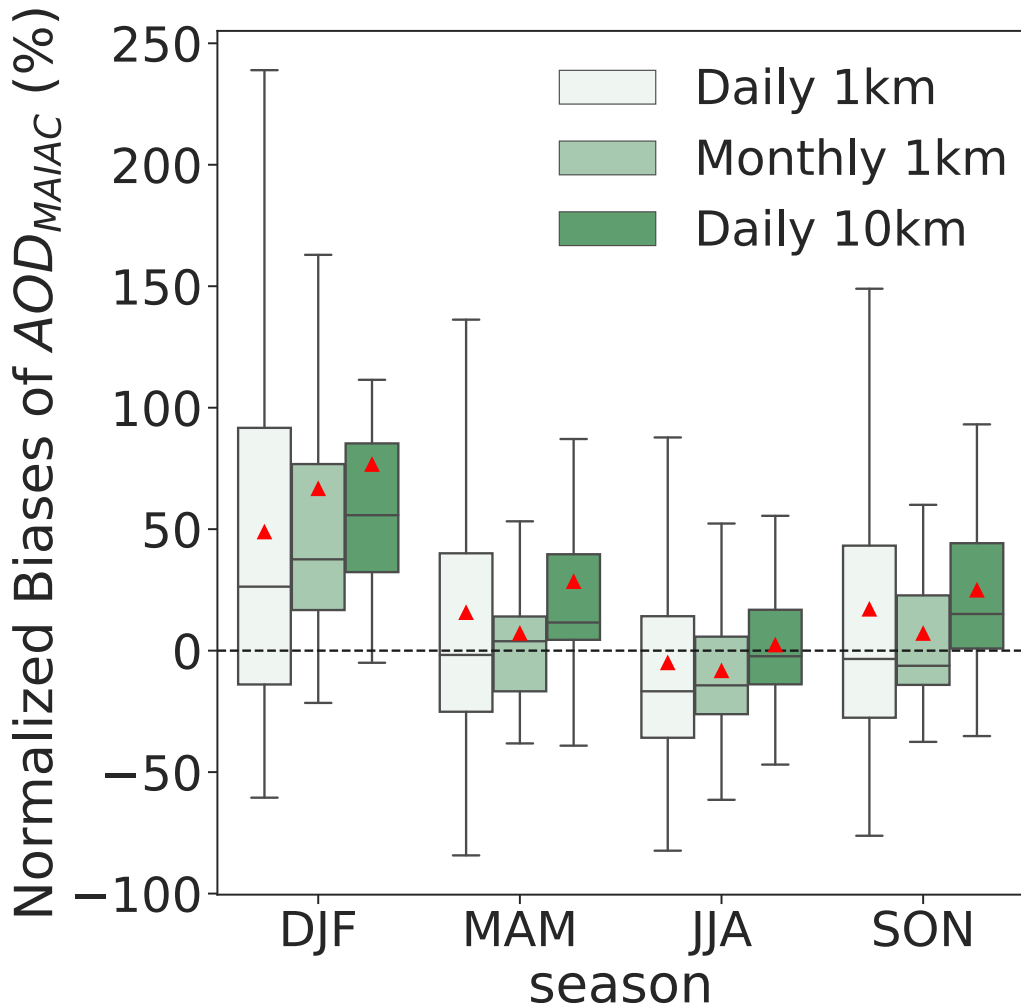
Figure 3 Distribution of normalized biases of AOD_{MAIAC} evaluated at 52 AERONET (including
DRAGON, only available for JJA) sites in four seasons of 2011 over the Northeast USA using
daily MAIAC AOD at 1 km resolution, 10 km resolution, and monthly average MAIAC AOD
composite (only including days when both satellite and AERONET measurements are available)
at 1 km resolution. The box shows the quantile range (IQR) while the whiskers extend to show the
rest of the distribution with outliers (points that are either 1.5×IQR or more above the third quantile
or below the first quantile) removed. The red triangles show the seasonal mean normalized biases.
Note that the normalized bias is an asymmetric metric, where model overestimates are unbounded
whereas model underestimates are bounded by -100%, therefore the mean of normalized biases is
typically higher than the median of the normalized biases.
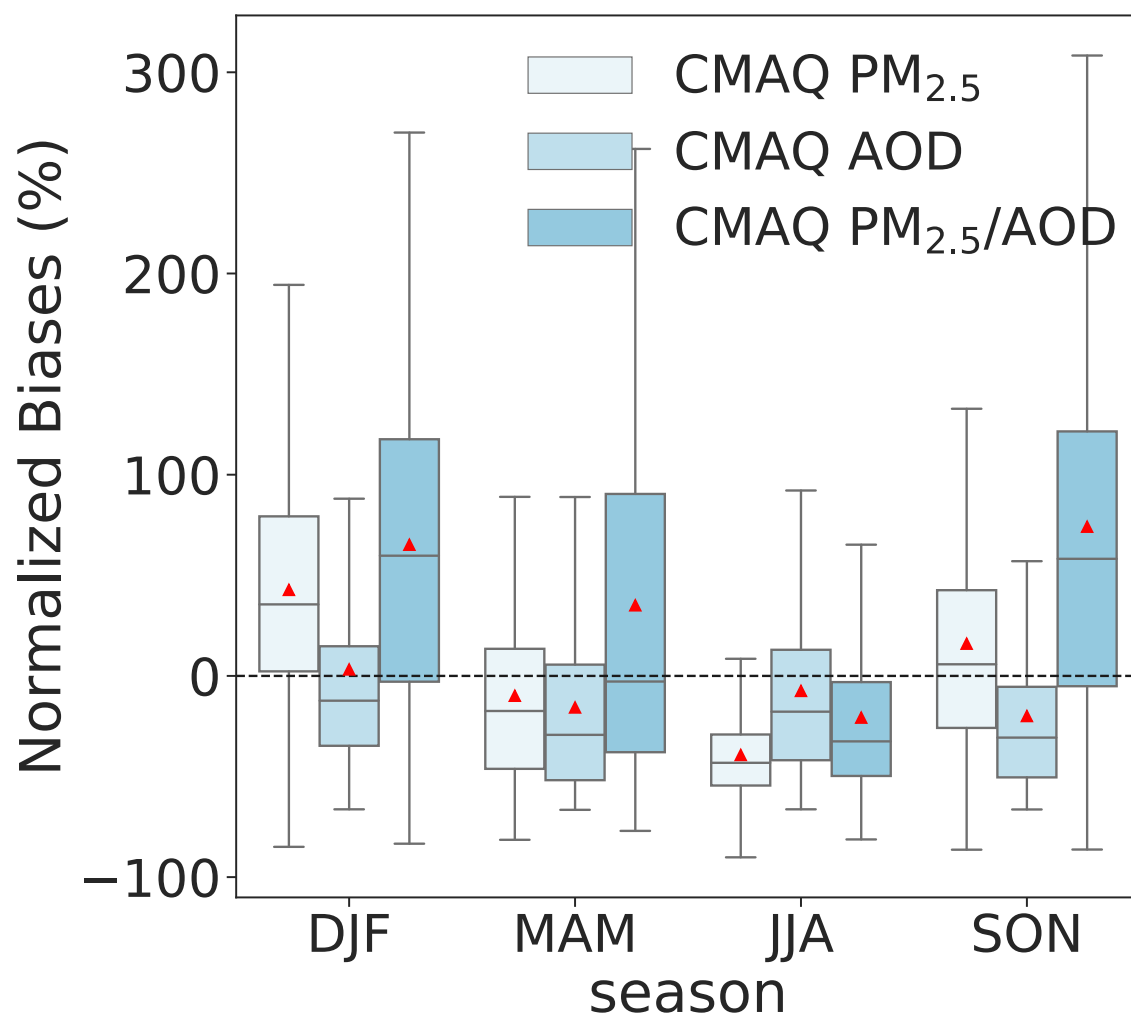
Figure 4 As in Fig. 3 but for daily $PM_{2.5\_CMAQ}$, AOD_{CMAQ}, and $PM_{2.5\_CMAQ}/AOD_{CMAQ}$ in each season of 2011 evaluated at 11 co-located AQS-AERONET sites over the Northeast USA.
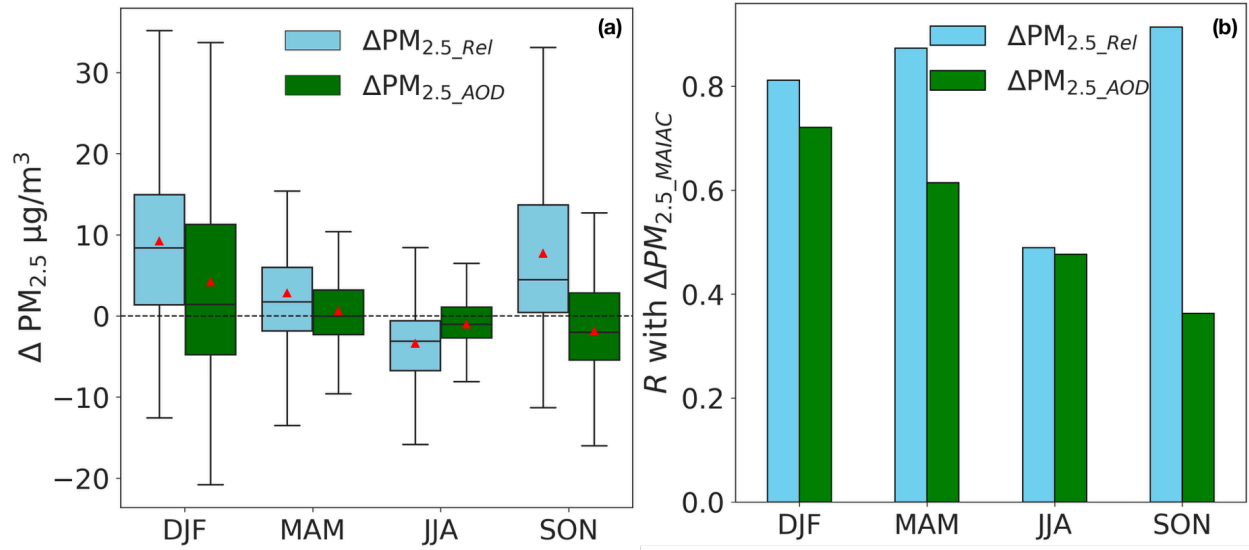
Figure 5 (a) Box plots comparing the distribution of biases in daily $PM_{2.5\_MAIAC}$ due to observational uncertainties in AOD_{MAIAC} (green, $\Delta PM_{2.5\_AOD}$) versus model uncertainties in $PM_{2.5\_CMAQ}/AOD_{CMAQ}$ (blue, $\Delta PM_{2.5\_Rel}$), evaluated consistently at 11 co-located AQS-AERONET sites over the Northeast USA. (b) Pearson correlation coefficient between the biases in daily satellite-derived $PM_{2.5}$ ($\Delta PM_{2.5\_MAIAC}$, evaluated with AQS observations) and the biases in $PM_{2.5\_AOD}$ attributed to observational uncertainties in AOD_{MAIAC} ($\Delta PM_{2.5\_AOD}$) versus model uncertainties in $PM_{2.5\_CMAQ}/AOD_{CMAQ}$ ($\Delta PM_{2.5\_Rel}$). $\Delta PM_{2.5\_AOD}$ is calculated by multiplying the biases of AOD_{MAIAC} with daily modeled $PM_{2.5}/AOD$ relationships (Eq. (8)). $\Delta PM_{2.5\_Rel}$ is calculated by multiplying the modeled $PM_{2.5}/AOD$ biases with daily AOD_{MAIAC} (Eq. (9)). The red triangles show the seasonal mean biases.
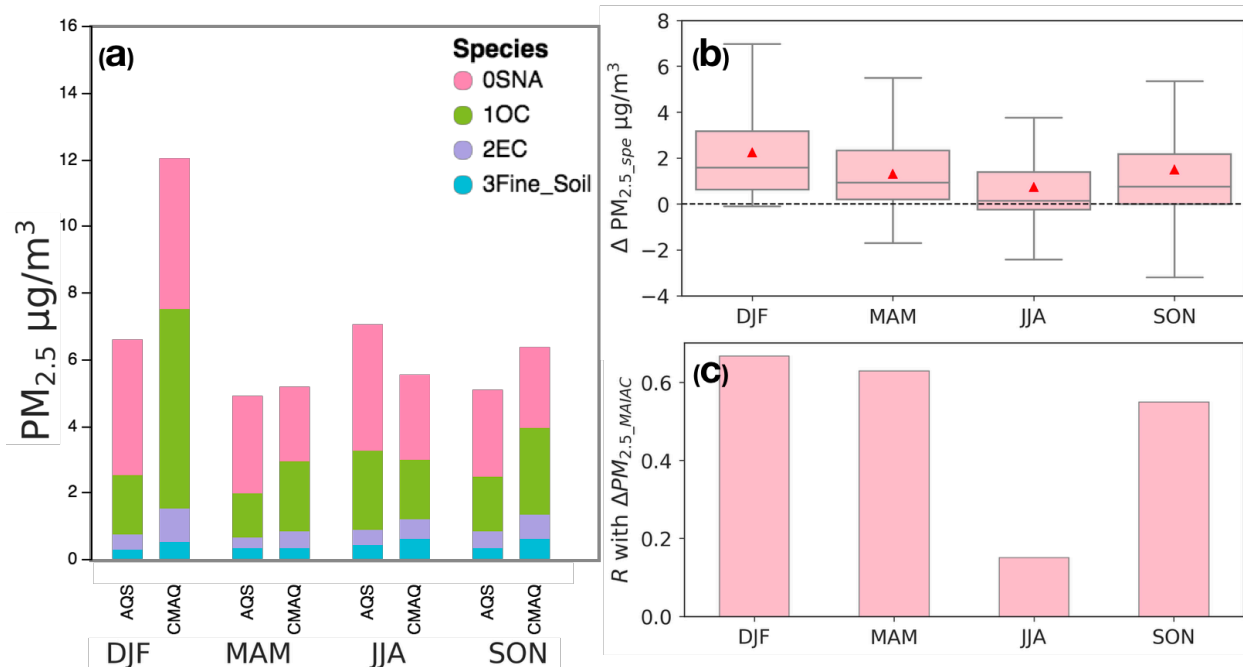
Figure 6 (a) Seasonal average PM$_{2.5}$ speciation from CMAQ vs. AQS observations in 2011 evaluated at 54 CSN and IMPROVE sites. (b) Box plots showing the distribution of estimated biases of daily satellite-derived PM$_{2.5}$ due to model biases in PM$_{2.5}$ speciation (ΔPM$_{2.5\_spe}$) by season for 2011. Red triangles show the seasonal mean biases. (c) Pearson correlation coefficient between the biases in PM$_{2.5\_MAIAC}$ (ΔPM$_{2.5\_MAIAC}$) and ΔPM$_{2.5\_spe}$.
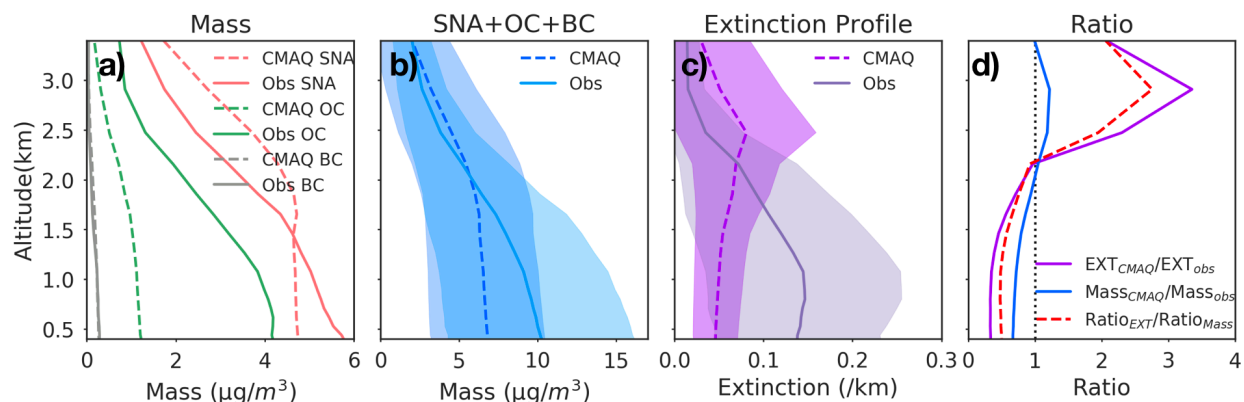
Figure 7 Campaign-mean vertical profiles of: (a) aerosol composition, (b) total mass (SNA+OC+BC), and (c) extinction from CMAQ vs. observations from the DISCOVER-AQ 2011 Baltimore-Washington D.C. campaign. (d) Campaign-mean vertical profile of the model-to-observation ratio of extinction ($Ratio_{EXT}$), total aerosol mass ($Ratio_{Mass}$) and $Ratio_{EXT}/Ratio_{Mass}$. Aircraft observations are first aggregated to match model layers, and corresponding model values are sampled concurrently with the time of observations. CMAQ modeled extinction is estimated with FlexAOD using the default parameters in Table 1. The shading in (b) and (c) shows the standard deviation of the day-to-day variability.
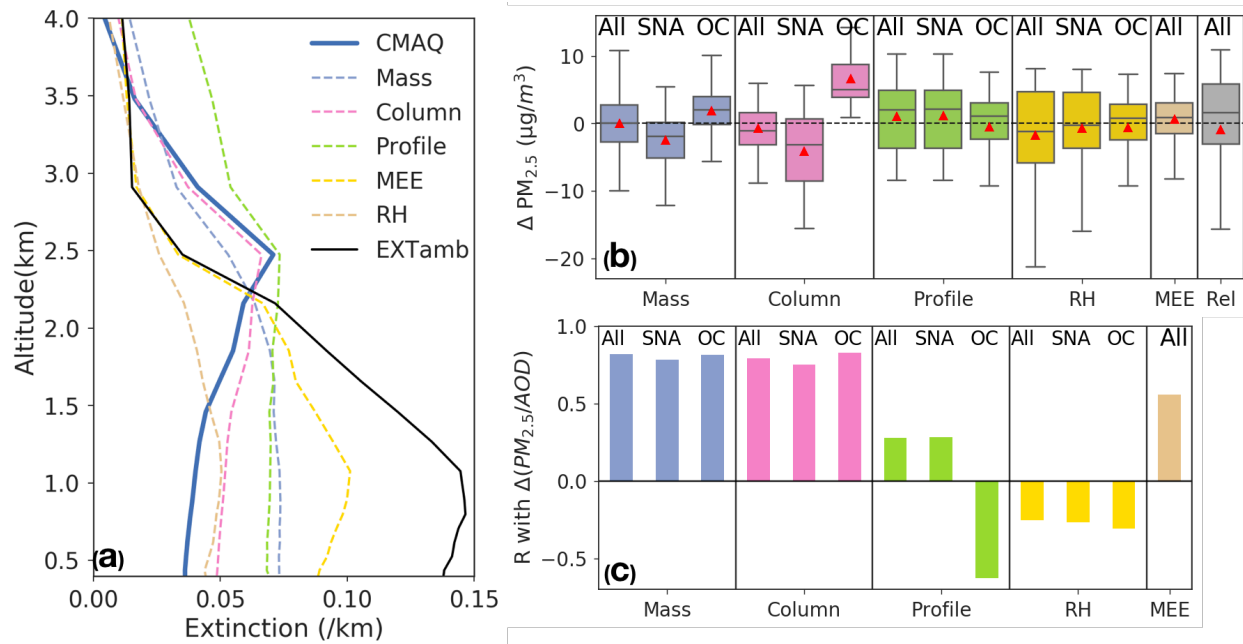
Figure 8 (a) Campaign-mean vertical profiles of extinction calculated from CMAQ speciated aerosol fields using FlexAOD, and that calculated by replacing modeled speciated aerosol mass (Mass), total column mass (Column), vertical profile shape (Profile), total mass extinction efficiency (MEE), relative humidity (RH) with that observed during DISCOVER-AQ 2011 Baltimore-Washington D.C. campaign. EXT_{amb} is the aircraft observed vertical extinction profile. (b) Box plots of the distribution of biases of $PM_{2.5\_MAIAC}$ attributed to each factor shown in (a), and the biases of $PM_{2.5\_MAIAC}$ attributed to modeled $PM_{2.5}$/AOD (Rel). Red triangles show the mean biases. (c) Pearson correlation coefficient between the biases in modeled $PM_{2.5}$/AOD relationships and the biases in modeled $PM_{2.5}$/AOD attributed to individual factors shown in (b).
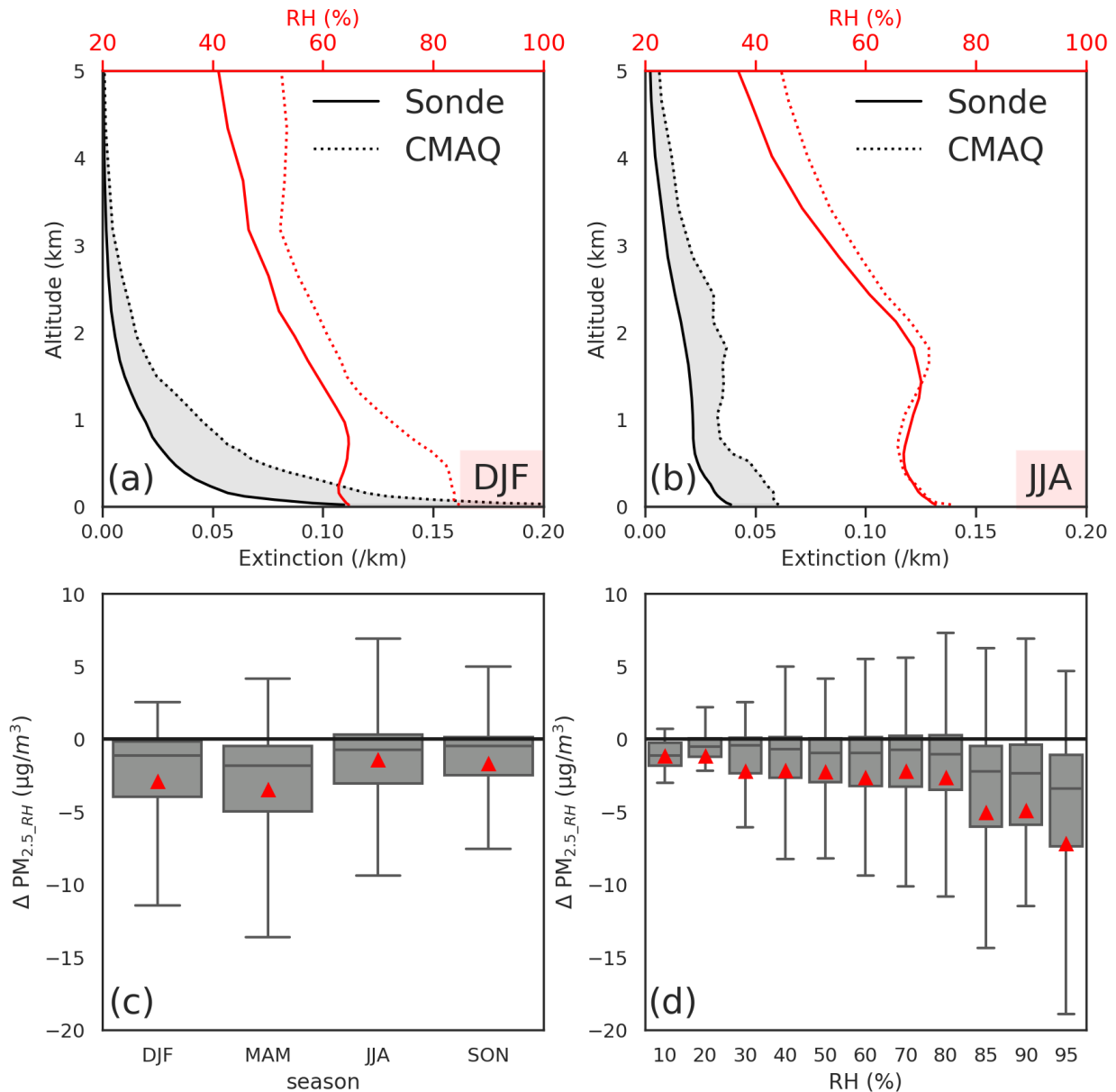
Figure 9 (a) DJF and (b) JJA average vertical profiles of the CMAQ modeled versus observed RH at 6 atmospheric soundings over the Northeast USA, and the modeled extinction versus that calculated by replacing modeled RH with observed values. The gray area shows the difference in extinction two profiles, with the total area being the difference in AOD. (c) Box plots showing the impacts of model bias of RH on the derived $PM_{2.5\_MAIAC}$ ($\Delta PM_{2.5\_RH}$) in four seasons of 2011, which are calculated by comparing the $PM_{2.5\_MAIAC}$ minus the one calculated using observed RH. (d) Box plots show the influence of model RH biases on the derived $PM_{2.5\_MAIAC}$ ($\Delta PM_{2.5\_RH}$) as a function of observed near-surface RH.
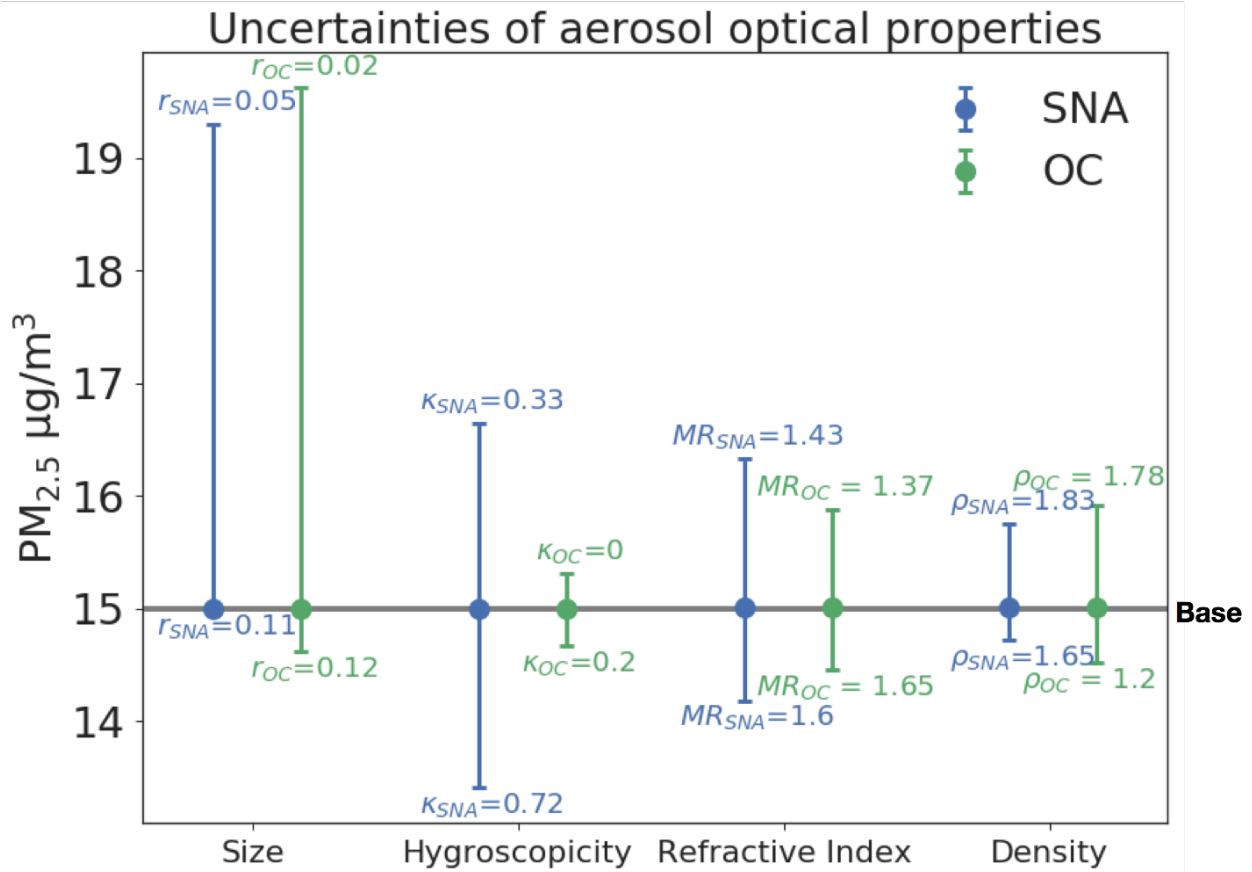
Figure 10 Uncertainties in annual average satellite-derived PM$_{2.5\_MAIAC}$ due to uncertainties of size distribution, hygroscopicity, refractive index and aerosol species density of sulfate-nitrate-ammonium (SNA; blue) and organic carbon (OC; green) sampled over AQS sites. The circle shows the annual average satellite-derived PM$_{2.5\_MAIAC}$ using the default parameters to calculate AOD$_{CMAQ}$ in FlexAOD (Table 1). The error bars represent the range of PM$_{2.5\_MAIAC}$ using different values for each parameter. The labels indicate the corresponding minimum or maximum parameter values that produce the range shown in PM$_{2.5\_MAIAC}$. The horizontal line at 15 µg/m^3 indicates the annual average PM$_{2.5\_MAIAC}$ calculated using default values for each aerosol optical property in the base FlexAOD.